Universidade de Aveiro
2008

Departamento de Electrónica,
Telecomunicações e Informática

Nefi Julião Carvalho

Impacto da Não-Linearidade em Arquitecturas de Sistemas de Telecomunicações Sem Fios

Impact of the Nonlinear Phenomenon on Wireless Radio Telecommunications Systems

dissertação apresentada à Universidade de Aveiro para cumprimento dos requisitos necessários à obtenção do grau de Mestre em Engenharia Electrónica e Telecomunicações, realizada sob a orientação científica do Dr. José Carlos Esteves Duarte Pedro, Professor Catedrático do Departamento de Electrónica, Telecomunicações e Informática da Universidade de Aveiro

o júri

presidente

Prof. Dr. João Nuno Pimentel da Silva Matos
professor associado do Departamento de Electrónica, Telecomunicações e Informática da Universidade de Aveiro

Prof. Dr. José Carlos Esteves Duarte Pedro
professor catedrático do Departamento de Electrónica, Telecomunicações e Informática da Universidade de Aveiro

Prof. Dr. Vitor Manuel Grade Tavares
professor auxiliar do Departamento de Engenharia Electrotécnica e de Computadores da Faculdade de Engenharia da Universidade do Porto

agradecimentos

Uma palavra de agradecimento ao grupo de Circuitos e Sistemas de Telecomunicações Sem Fios do Instituto de Telecomunicações de Aveiro em especial ao Professor José Carlos Pedro pela sua incondicional disponibilidade e apoio em todo momento.

De uma forma geral agradeço a todos os que me apoiaram durante o decurso do trabalho quer voluntariamente quer institucionalmente, em especial ao Instituto de Telecomunicações e á empresa Space Services, Lda.

palavras-chave

Co-Simulação, Distorção Não-Linear, Circuitos Rádio Frequência, Sistemas de Telecomunicações Sem Fios.

resumo

A dimensão e heterogeneidade de recentes sistemas de telecomunicações sem fios impossibilitam a previsão do comportamento do sistema completo quando operado nos limites das suas capacidades. Isto torna irrealista o estudo do impacto do fenómeno não linear no desempenho dos sistemas em especial devido a que os resultados são diferentes quando estudados em separado ou embebidos num sistema. Este trabalho ultrapassa estas problemáticas através do uso de técnicas de co-simulação e de modelação do actual estado da arte as quais tornam possível uma representação mais realista do desempenho de um sistema.

acknowledgements

A Word of acknowledge to the Wireless Circuits and Systems Group from the Instituto de Telecomunicações Aveiro, and especially thanks to Professor José Carlos Pedro for his unconditional openness and support at all moment.

In general, I would like to thanks to all who supported me during this work either voluntary or institutionally, especially to Instituto de Telecomunicações Aveiro and to the company Space Services, Lda.

keywords Co-Simulation, Nonlinear Distortion, Radiofrequency Circuits, WLAN Systems

abstract The dimension and heterogeneity of recent wireless radio telecommunication systems makes impracticable the prediction of the full system behavior when pushed to its performance limits. This makes unrealistic the study of the impact of the nonlinear phenomenon on the systems performance, especially because the results are different when studied alone or embedded in a system. This work overcomes these difficulties by using state-of-the-art co-simulation and modeling techniques that made possible the presentation of more realistic system performance evaluations.

Table of Contents

List of Figures

List of Tables

List of Acronyms

ACPR – Adjacent Channel Power Ratio

ANSI – American National Standards Institute

BER – Bit Error Rate

CCK – Complementary Code Keying

CCPR – Co-Channel Power Ratio

CCDF – Complementary Cumulative Distribution Function

CDMA – Coded Division Multiple Access

CE – Circuit Envelope Simulation

CSMA/CA – Carrier Sense Multiple Access – Collision Avoidance

DC – Direct Current

DSSS – Direct-Sequence Spread Spectrum

DUT – Device Under Test

EIRP – Equivalently Isotropic Radiated Power

ETHB – Envelope Transient Harmonic Balance

EVM – Error Vector Magnitude

FER – Frame Error Rate

FOM – Figure of Merit

GaAs – Gallium Arsenide

ISM – Industrial, Scientific and Medical Radio Band

KCL - Kirchhoff's Current Law

LNA – Low Power Amplifier

LTVS – Liner Time Variant System

MAC – Media Access Control Layer

Mbps – Mega Bits Per Second

Mcps – Mega Chips Per Second

Msps – Mega Samples Per Second

NLTF – Non Linear Transfer Function

OFDM – Orthogonal Frequency-Division Multiplexing

PA – Power Amplifier

PER – Packet Error Rate

PHEMT – Pseudomorphic High Electron Mobility Transistor

PLCP - Physical layer Convergence Procedure

PN – Pseudo Noise

PSDU – PLCP Service Data Unit

RMS – Root Mean Square

SDF – Synchronous Dataflow

TSDF – Timed Synchronous Dataflow

UMTS – Universal Mobile Telecommunications System

WLAN – Wireless Local Area Network

Chapter 1

Introduction

The nonlinear phenomenon in telecommunications circuits is a widely studied theme due to its considerable constraints on our “mobile wireless age” terminals. Factors such as power consumption or autonomy and data rate are directly limited or dependent from nonlinear effects to mobile terminals. However, the nonlinear mathematical modeling complexity, its simulation and the methods to obtain the solutions namely the circuit’s outputs, are often factors moving design engineers to bypass the problem consequently reducing system performance.

Recent wireless radio telecommunications systems are pushing the technology limits demanding higher transmission bandwidths with higher spectral efficiency. This requires the capability to handle exceptionally high amounts of data and its treatment in order to correctly represent and simulate the whole system behavior. Therefore, the dimension and heterogeneity of recent electronic circuits makes it difficult to simulate the wireless radio system at once. An appropriate mixture of state of the art techniques is required to represent the system behavior, especially because is expected that the nonlinear phenomenon impact will be distinct when studied alone or if embedded in a system.

Co-simulation methods applied on telecommunication systems are a recent research subject with increasing importance. It has arisen with an increased interest with recent developments on simulation methods based on system and excitation description within two time-domain scales [1, 2]. In fact, when applying these methods to nonlinear circuit simulation would transform a problem of solving time-domain nonlinear ordinary differential equation (ODE) in another problem whose representation is based on differential equations to the partial derivatives [3, 4] in two or more time-domain virtual scales. This way, a substantial improvement on computational efficiency is achieved.

Co-simulation scheduling methods based on Berkeley Ptolemy [5] are being improved and became recently available on commercial platforms. Considerable improvements where achieved handling the dataflow and interfaces between N-dimensional space signals and systems. These methods enable the cascade and concurrent simulation of blocks with different algorithms according to the most appropriate method for each circuit block by shrewdly interfacing signals and its rates.

These methods have clear advantages on the simulation of nonlinear radiofrequency and microwave circuits [3, 7-11], but only recently are being applied to the study of the impact of this type of distortion phenomenon in wireless telecommunications circuits [12-14].

1.1. Objectives

This work addresses the problem of accurately and timely efficient prediction of a wireless radio system nonlinear response to a real excitation signal. Avoiding the traditional approach of using high-level simplification methodologies and maintaining or increasing the results' accuracy, the system simulation turns on a high complexity mix of state of the art technologies and techniques. The main objective is the study and production of the appropriate platforms making use of state of the art simulation and modeling techniques to achieve demonstrative nonlinear system impact analyses. The identification of aspects regarding nonlinear identification and characterization, nonlinear simulation, signal representation, signals interfacing are subjects considered on this study.

As the nonlinear behavior presented by the transmitter power amplifier in actual wireless radio systems is the bottleneck for its performance improvement, the analyses are centered on this block.

Due to the nature of the nonlinear phenomenon, the only consistent way to perform this study is exciting the system nonlinear block with the most realistic and appropriated representation of the real transmitted signals, i.e. band pass modulated data. This implies the development of a simulation setup using the most recent techniques of co-simulation and nonlinear modeling in order to comply with acceptable results precision and affordable computational requirements. Additionally, a power amplifier was developed in order to study the main nonlinear signal distortion generation block model.

1.2. Thesis Outline

This Thesis document starts by identifying and locating the nonlinear distortion effects whose impact is predominant on the selected wireless radio telecommunication systems architectures. This is addressed on Chapter 2. starting with a theoretical overview of the nonlinear phenomenon and the identification of its main sources on two recent Wireless Local Area Network (WLAN) system architectures. Here are described the architectures of CDMA and OFDM spread spectrum systems such as IEEE 802.11b and 802.11a, respectively, particularly selected due to its novelty and interest on impact of nonlinearities on its modulation principles. Considering that the propagation channel significantly affects the wireless transmitting performance, a briefly explanation is presented screening how recent systems overcome its impairments.

To efficiently and precisely compute the realistic performance of all the blocks within the systems, each block has to be modeled and simulated. These simulation techniques and their particularities are presented on Chapter 3. All simulations and platforms were developed under Agilent Advanced Design System software platform. Special attention is reserved for the transmitter Power Amplifier (PA). This block needs to be carefully modeled and simulated in order to precisely output its real nonlinear performance.

The characterization and selective validation of the simulation models and platform used is stated at Chapter 4. A synthesized description of the models performance and designs behavior, from device to system level, is presented in view of the main objectives of the analyses proposed. Additionally, the signal quality analysis characterization and signal interfaces considered are presented.

Demonstrative examples of inband and outband nonlinear distortion impact are shown on Chapter 5 presenting the developed appropriate platforms and case studies. The quantification of nonlinear distortion generation and nonlinear distortion adjacent spectrum impact are presented.

Finally, on Chapter 6 the author draws some conclusions and remarks considering the results achieved and the work performed.

Chapter 2

Signal Distortion in Wireless Radio Systems

Two main different types of signal perturbation can be distinguished. One is generated independently from the information signal like system's internal or external noise and also other interfering signals such as other systems operating on the same channel. Another type of signal perturbation is generated as a function of the transmitted information signal. This latter is called distortion as it modifies the information signal as a consequence of its characteristics.

Some kinds of signal distortion are not problematic for telecommunications systems such as scale or offset changing. This type is referred as linear distortion regarding the nature of the transformation that was applied to the signal. Being a linear transformation, the signal can be restored by applying the reverse transformation to the one which distorted the signal. On the other hand, there are nonlinear signal transformations that can result in scale, shape and/or even the generation of new not correlated components designated as nonlinear signal distortion.

On this Chapter it is first presented a brief description and characterization of the nonlinear distortion phenomenon and introduced the appropriate mathematical descriptions to reproduce the nonlinear behavior sources. Additionally, these main sources of nonlinear behavior are identified within a typical architecture of a wireless radio telecommunication

system. Finally, the impact of the wireless radio channel on the transmitted signal is approached.

2.1. Nonlinear Distortion Fundamental Concepts

The nonlinear function is, by definition, a function that does not obey the superposition condition. In fact, strictly speaking, there is not any real linear system considering that there are always limitations on all real systems. Nevertheless, under particular and restricted operation conditions, real systems are treated as being linear considering that the nonlinear influence is inconsequential to the final output. This linearity assumption avoids complex and sometimes unworkable design particularities although frequently originating reduced performance final design solutions.

Taking into consideration that no matter how complex a signal waveform is, it can be recreated by combining a number of continuous sine waves (tones) with appropriate different frequencies, phases and amplitudes. An representation of the transmitted envelope by a group of unmodulated carriers – a multitone excitation can be represented as $x(t)$:

$$\text{(Eq.1)} \qquad x(t) = \sum_{q=1}^{Q} A_q \cos(w_q t + \theta_q) \text{, with } w_q = w_0 + (q-1)\Delta w$$

Being $x(t)$ a general information signal represented by a Q equally spaced tones and A_q the amplitude of each tone. The tones are of frequencies w_q equally spaced by Δw starting from frequency w_o. Not of minor importance is each single tone's phase θ_q, their values will contribute to the definition of the signal envelope and consequently affecting the system nonlinear behavior. The parameters that best approximate this result would be considering randomly distributed values of the tones phases' θ_q.

A general common representation of a weak nonlinear system output can be a polynomial truncated to the 3rd degree:

(Eq.2) $$y_{NL}(t) = a_1 x(t) + a_2 x(t)^2 + a_3 x(t)^3 + \ldots$$

This system representation is commonly selected regarding that it can, with reasonable accuracy, reproduce most electric systems behavior and nonlinearities having also the advantage that the first order term directly corresponds to the system behavior operating in its pseudo linear conditions. A common assumption is to truncate the system representation to the 3rd order regarding that the higher order terms will have a considerable lower impact. The third order impact will limit the system power reducing higher order major effects.

Using the nonlinear system from (Eq.2) and applying the mutitone signal excitation (Eq.1) the response is another mutitone type signal with new mixing (intermodulation) nonlinear products of the input tones. The component of $y_{NL}(t)$ centered at frequency $w=w_{q1}+\ldots+w_{qn}$ due to the intermodulation of input components can be expressed [18][19] as:

(Eq.3) $$y_{n,w}(t) = \sum_{w_{q1}+\ldots+w_{qn}=w} \frac{a_n}{2^{n-1}} \binom{n}{n_{-q},\ldots,n_q} \prod_{i=1}^{n} A_{q_i} \cos(w_{q_i} t + \theta_{q_i})$$

Where $w = \sum_{q=-Q}^{Q} n_q w_q = \sum_{i=1}^{n} w_{q_i}$, $\sum_{q=-Q}^{Q} n_q = n$ and $\binom{n}{n_{-K},\ldots,n_K} = \frac{n!}{n_q!\ldots n_{-q}!}$ is the multinomial coefficient. The output tone frequencies are located at all possible combinations of all individual input tone frequencies.

This corresponds to the addition of new spectral components to the excitation signal frequently referred as spectral regrowth. The new generated spectral components are located at base band, at the harmonics of the excitation, near the excitation and also co-located with the excitation band as represented at Fig. 1.

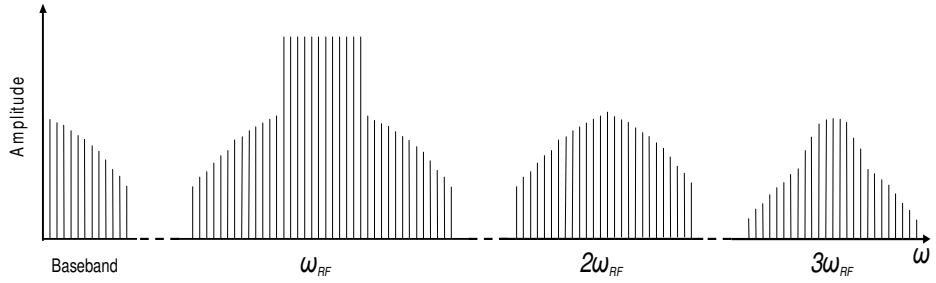

Fig. 1. Spectrum response of a third order nonlinear system to a general narrowband multitone excitation

As the distortion located at the excitation harmonics and DC are distant (in frequency) from the excitation, they can be filtered and easily surpassed by the systems. Nevertheless, the distortion located near the excitation signal – Intermodulation - cannot be completely filtered and so is the main distortion problem. This work is focused on the Intermodulation distortion effects regarding that it directly determines the systems performance in presence of distortion phenomena's. On the next figure can be seen the detail of the input and output spectrum generated by a nonlinear power amplifier when excited by a multitone signal.

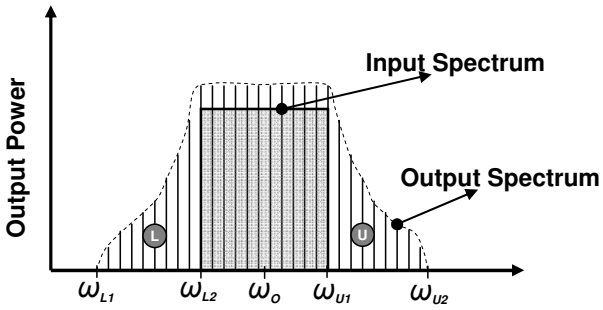

Fig. 2. Input and output spectra as observed in a system excited by a narrowband multitone signal

2.1.1. Intermodulation Distortion Characterization

In order to quantify the nonlinear phenomenon, different characterization measurements and figures of merit (FOM) are specifically defined. These possibilities electronic systems evaluation mainly intended for power amplifier and mixer's nonlinear performance analysis. The most realistic stimulus for intermodulation distortion characterization is the real information signal. Although, the equipment to provide this kind of signal excitation is

not always available and requires expensive equipment setups. Therefore, signal approximations and simpler figures of merit were created in order to present a quick estimation of the element nonlinear behavior.

One Tone Characterization

Although not directly measuring Intermodulation distortion, the one tone setup is presented due to its major importance as a first analysis approach of the nonlinear behavior of a device. It consists on the variation of one input tone amplitude and the verification of the correspondent device under test (DUT) output tone power and relative phase. With this test, figures such as gain variation (AM/AM) and amplitude to phase conversion (AM/PM) are obtained. Important to verify with this setup is the gain compression and phase distortion as function of the input signal power. From those measurements are extrapolated figures such as the 1dB gain compression point (P1dB) which represents the output power level at which the output signal is 1dB below to an linearly extrapolated extension (Fig. 3 – dashed with label 1st order) of the first order or linear term.

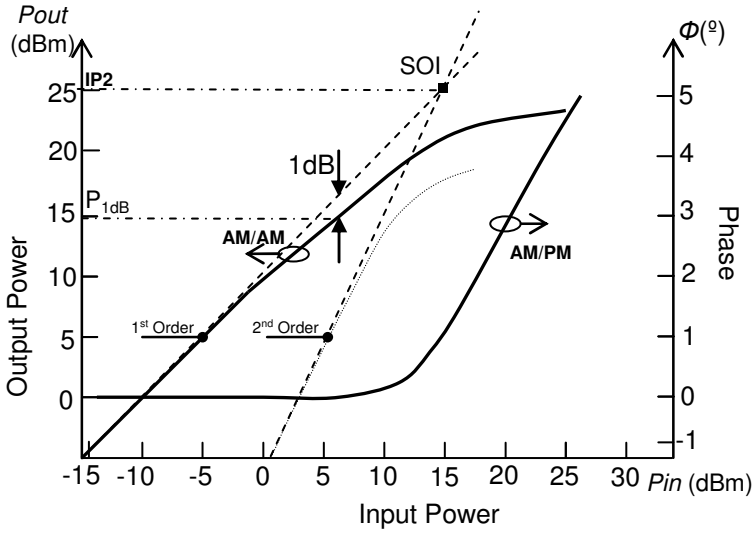

Fig. 3. One tone nonlinear test outputs: AM/AM conversion, AM/PM conversion, SOI and P1dB

Beyond the 1dB compression point the conversion loss is higher increasing the power converted into heat and higher order harmonics. In addition, the phase will be more

affected and very much dependent of minor input power variations, a fact that reduces considerably the performance of digitally modulated signals.

Nevertheless its simplicity, the one tone test is important for the nonlinear element evaluation considering that it allows a coarse prediction of the level of phase and amplitude nonlinear influence on the signal and thus the system performance.

Two Tone Characterization

The most common setup for Intermodulation distortion analysis consists on the excitation of the DUT with two tones - fundamentals. In addition to the harmonics measurements possible by one tone setup, this setup provides also the analysis of the mixing products generated as represented on Fig. 4.

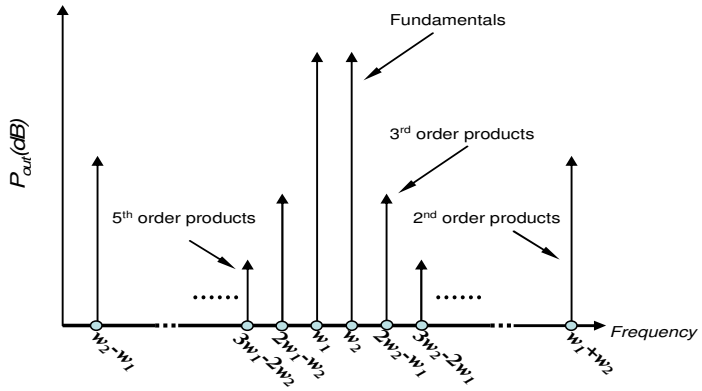

Fig. 4. Two tone excitation output from a nonlinear device test

The most widely used intermodulation distortion characterization standard is the third order interception point (TOI) and its respective output level referenced as IP3. The TOI is defined to be the intersection of the first and third order linear extrapolations from the fundamental tones and the intermodulation products respectively. Arbitrary n^{th} order intercept points may also be defined in an analogous manner.

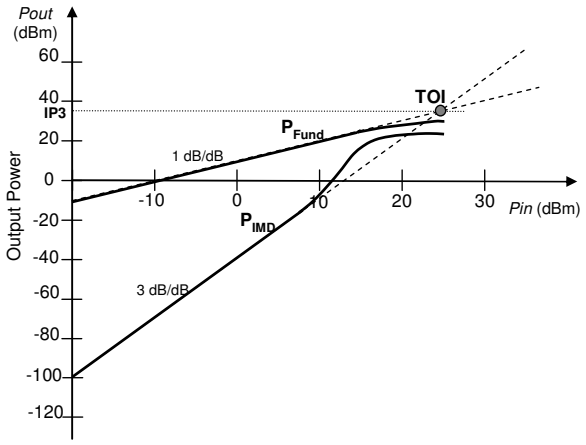

Fig. 5. Third order nonlinear characteristic, TOI and IP3 figures of merit

A high level intercept point indicates a high suppression of undesired intermodulation products. The TOI is an important measure of the system's linearity over the desired range of output power levels.

Multitone, White Noise and Continuous Spectra Characterization

In order to characterize the in band distortion and analyze the spectral regrowth more dense stimulus are required. This is the case of Multitone excitation as a representation of the signal over its bandwidth. It enables the estimation of in band distortion products generated by the self-mixing of multiple signal band spectral components.

The Multitone excitation is a signal representation composed by a set of equally spaced tones with random phases occupying the spectrum of the band of interest as presented on the input spectrum from Fig. 2. However, special attention must be taken with the relative phase of the tones realizing that different phase combinations generate considerably different signal envelopes and then producing different distortion behavior. A generalization of multitone is the White Noise excitation that consists on the generation of a random signal with flat power density over the band of interest to stimulate the nonlinear DUT.

An important metric for the intermodulation characterization is the Adjacent-Channel Power Ratio (ACPR). It is widely used on modern digital radio telecommunication systems analysis once it provides a good estimate of the distortion power interference on the signal adjacent channels. ACPR is defined as the ratio of the integrated signal power to the two adjacent upper and lower channels band integrated power, as:

(Eq.4)
$$ACPR \equiv \frac{\int_{w_{L_2}}^{w_{U_1}} S_o(w)dw}{\int_{w_{L_1}}^{w_{L_2}} S_o(w)dw + \int_{w_{U_1}}^{w_{U_2}} S_o(w)dw}$$

being S_o the power spectral density function of the system output and the *Lx*, *Ux* the band limits of the lower and upper adjacent channels respectively. When applied to a multitone excitation on the ACPR (Eq.4) the integrals turn into summations of the respective band tones and intermodulation products power.

Finally, an in-band nonlinear distortion metric is the Co-Channel Power Ratio (CCPR). The CCPR is defined as the ratio of integrated channel power to the integrated in-band perturbation power.

(Eq.5)
$$CCPR \equiv \frac{\int_{w_{L_2}}^{w_{U_1}} S_o(w)dw}{\int_{w_{L_2}}^{w_{U_1}} S_{yy}(w)dw}$$

Being SS_{yy} the in-band perturbation power spectral density function.

The CCPR metric, in contrast to noise power ratio (NPR), considers the in band perturbations being or not correlated to the input signal. This option was selected considering that the performance of the wireless radio system will be affected also by the signal correlated nonlinear distortion products such gain compression/expansion and phase variation.

2.2. Wireless Radio Telecommunications Systems Architecture

As referred on previous points, the nonlinear phenomenon affects the system performance as function of the instantaneous power of the signal excitation. This instantaneous power will be mainly defined by the signal modulation and signal conditioning operations.

Considering the use of samples from actual telecommunications industry and the best possible variations on signal envelope behavior, this study selected two systems with different second level modulation techniques both based on frequency spreading. The selected spreading methodologies considered were the Direct-Sequence Spread Spectrum (DSSS) and Orthogonal Frequency-Division Multiplexing (OFDM). On these wideband frequency diversity techniques, or spread-spectrum techniques, the signal bandwidth is much larger than the user channel data rate. These techniques are targeted to exploit the frequency selectivity fading characteristic of the radio propagation channel.

A general block diagram of recent wireless radio system is presented on Fig. 6. The information is properly prepared to overcome the physical transmitting environment but at the end of the chain the end-user transparently receives the information.

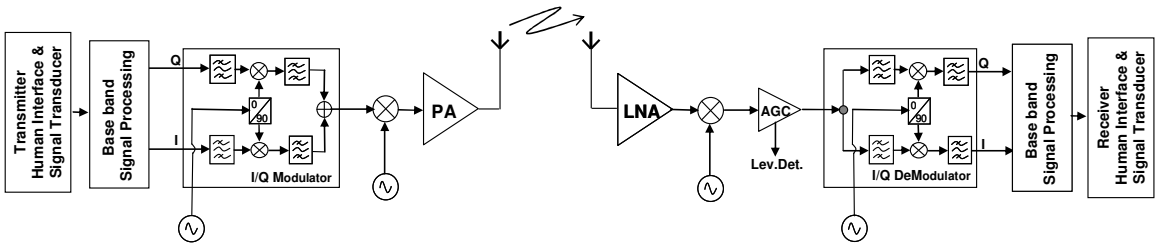

Fig. 6. General wireless radio telecommunications system block diagram

Most operations on the information signal are by their nature linear or if even nonlinear are reversible and intentional. Signal transformations such as coding, modulation, spreading, frequency conversion, filtering and amplification are conditioning operations in order to overcome the physical impairments of the transmitting medium, specially the propagation channel.

With recent technology advances in velocity improvement of Digital Signal Processing (DSP) devices, the telecom systems tend to be digital as much as possible. This kind of digital circuitry can achieve a very high performance with no distortion considering the digital philosophy. However, a few blocks still need to be analog due to the interface with the real propagation medium.

The analog blocks/elements that can produce nonlinear distortion components over the signal can be: frequency conversion, signal level conversion, antenna and propagation channel. Although all these analog blocks can generate nonlinear distortion components, the transmitter power amplifier plays the most critical role. The power amplifier needs to increase significantly the signal level to overcome the propagation channel and transmission distance. This generally makes of the power amplifier one of the most power consuming blocks of wireless systems, which are mostly battery powered. In addition, this block has commonly the lowest power efficiency regarding that the increase in efficiency inevitably leads to the increase of nonlinear distortion effects. Being then the power amplifier as the bottleneck of wireless mobile systems regarding autonomy and efficiency and thus selected as the target study block on this work.

Frequency up and down converter blocks, digital to analog and analog to digital converters and antennas from the transmitter and receiver blocks can also introduce nonlinear distortion to the signal but were not considered on the scope of this work.

The low noise amplifier (LNA) block at the receiver will also generate nonlinear distortion effects. Regarding the low signal level and low power requirements from this block, it is commonly operated at restricted quasi-linear modes that significantly reduce the nonlinear constraints over the signal. The major impact of this block appears when at the receiver LNA high power adjacent channel interferer signals are also amplified generating nonlinear cross-modulation products. This impact can be minimized using better receiver input filtering increasing the receiver selectivity. The impact of the nonlinear distortion generated at the receiver and thus at the LNA was not considered on this work.

2.2.1. Direct-Sequence Spread Spectrum Technology

Direct-sequence spread spectrum (DSSS) can be considered as a second level modulation technique widely used on mobile phone networks (CDMA2000, UMTS, WCDMA) and in wireless local area networks (WLAN). On this study it was selected a wideband system with high modulation efficiency in order to evaluate its performance under a nonlinear distortion element – IEEE Std 802.11b-1999 (R2003) (Supplement to ANSI/IEEE Std 802.11, 1999 Edition).

The IEEE Std 802.11b-1999 (R2003) supplement, hereafter referred as 802.11b, enhanced the initial standard with a Higher-Speed Physical Layer Extension clause which turn this standard able to allow WLAN up to 11Mbit/s bitrate. This enhancement considers the use of Complementary Code Keying (CCK) modulation scheme that is a derivation from DSSS, with the main difference being the spreading codes used although maintaining the same architecture. The standard allows versatile modes of operation regarding the possibility of switching between several bitrate according to the transmitted BER performance and thus varying the modulation efficiency.

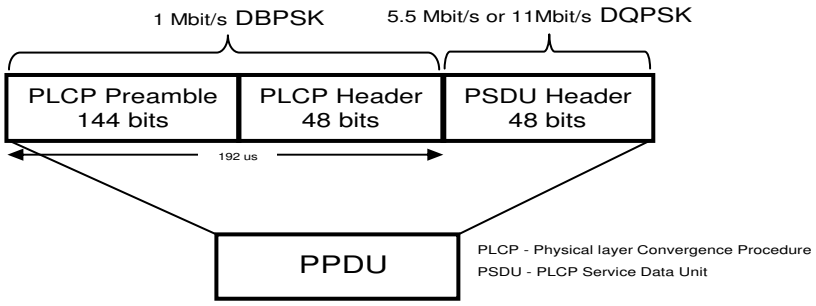

Fig. 7. Detail of MAC layer showing the modulation under a 802.11b data frame [26]

CCK is a variation on M-ary Orthogonal Keying modulation, which uses I/Q modulation architecture with complex symbol structures. The channel orthogonality is achieved by a set of Walsh/Hadamard functions known as Complementary Codes. This complex modulation architecture generates a signal waveform whose characteristics are of main interest to the nonlinear distortion analysis impact over the transmission chain.

To assure that the modulation has the same bandwidth as the previous existing 802.11 DS modulation, the chipping rate is kept at 11 Mcps while the symbol rate is increased to 1.375 Msps. This accounts for the shorter symbols and makes the overall bit rate 11 Mbps.

The standard specifies the maximum allowable output power according to each geographical zone as in Table. 1.

Table. 1. IEEE 802.11b Transmit power levels

Maximum output power	*Geographic location*	*Compliance document*
100 mW (EIRP)	Europe	ETS 300-328
10 mW/MHz	Japan	MPT
1000 mW	USA	FCC15.247

This 802.11b standard was specified for the 2.4 GHz band designated for Industrial Scientific and Medical (ISM) applications. The correspondent IEEE transmission spectral mask is shown at Fig. 8. The measurements shall be made using a 100 kHz resolution bandwidth and a 100 kHz video bandwidth [26].

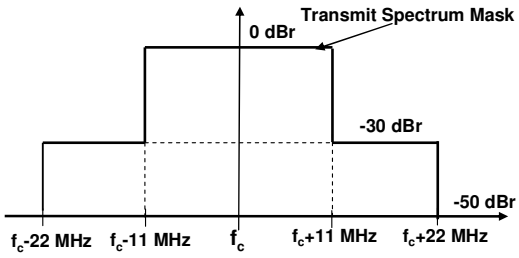

Fig. 8. IEEE 802.11b Transmit Spectrum Mask (*fc* is the channel center frequency)

2.2.2. Orthogonal Frequency-Division Multiplexing Technology

Recent technology advances in digital signal processing hardware platforms permitted the use of more complex modulation schemes. Orthogonal frequency-division multiplexing (OFDM) is considered, by some industry players, as integrant of the 4th generation of wireless telecommunications. It can be considered as a second level modulation with good robustness to multipath echoes, which is typical on the indoor and mobile environments.

On this work, the selected OFDM representative system was the IEEE Std 802.11a-1999 (R2003) (Supplement to ANSI/IEEE Std 802.11, 1999 Edition). On this system, each OFDM symbol is composed of 52 subcarriers, of which 48 carry data and 4 subcarriers serve as phase reference pilots. The specifications of the Physical Layer encompass data rates from 6 Mbit/s up to 54 Mbit/s, with 20 MHz spacing between adjacent channels. The range of data rates is provided to match the wide range of radio channel characteristics in both indoor and outdoor environments.

Table. 2. Bit rate, modulation and coding rate possibilities for IEEE 802.11a Systems [27]

Data rate (Mbit/s)	*Modulation*	*Coding rate*	*Data rate (Mbit/s)*	*Modulation*	*Coding rate*
6	BPSK	½	24	16-QAM	½
9	BPSK	¾	36	16-QAM	¾
12	QPSK	½	48	64-QAM	$^2/_3$
18	QPSK	¾	54	64-QAM	¾

This standard allows a multirate mechanism at the medium access control level (MAC) which ensures that the devices communicate with each other at the best data rate real time in harmony with the propagation channel conditions.

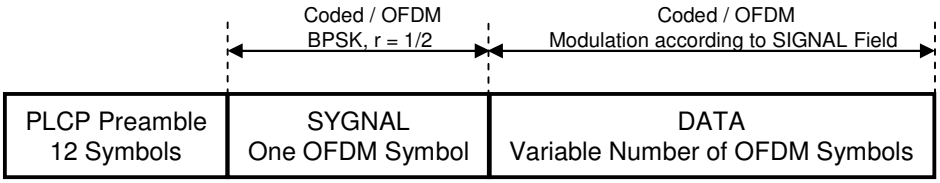

Fig. 9. Detail of MAC layer showing the modulation under a 802.11a data frame [27]

Dependent on the data rate active on each transmission, the standard defines different signal quality specifications requirements in terms of maximum outband adjacent spectrum generation (spectral regrowth) and also in terms of transmitter maximum allowed constellation error.

Table. 3. **Allowed relative constellation error versus data rate***

Data Rate (Mbit/s)	*Relative Constellation Error (dB)*	*Relative Constellation Error (%RMS)*	*Data Rate (Mbit/s)*	*Relative Constellation Error (dB)*	*Relative Constellation Error (%RMS)*
6	-5	56.2	24	-16	15.8
9	-8	39.8	36	-19	11.2
12	-10	31.6	48	-22	7.9
18	-13	22.3	54	-25	5.6

* - Information from the IEEE802.11a-1999 standard, Section 17.3.9.6.3

The relative constellation RMS error, averaged over subcarriers, OFDM frames, and packets shall not exceed a data-rate dependent value according to Table. 3.

The 802.11a system operates in the 5 GHz band, as allocated by a regulatory body in its operational region. Spectrum allocation in the 5 GHz band is subject to authorities responsible for geographic-specific regulatory domains (e.g., global, regional, and national). Other different bands are open for operation with different power limitations according to the regulatory bodies.

The standard specifies the maximum allowable output power according to each geographical zone as in Table. 4.

Table. 4. **Maximum TX power levels – For the Unit States**

Frequency Band (GHz)	*Maximum output power with up to 6 dBi antenna gain (mW)*
5.15 – 5.25	40 (2.5 mW/MHz)
5.25 – 5-35	200 (12.5 mW/MHz)
5.725 – 5.825	800 (50 mW/MHz)

The spectrum mask defined for the 802.11a system is as the Fig. 10.

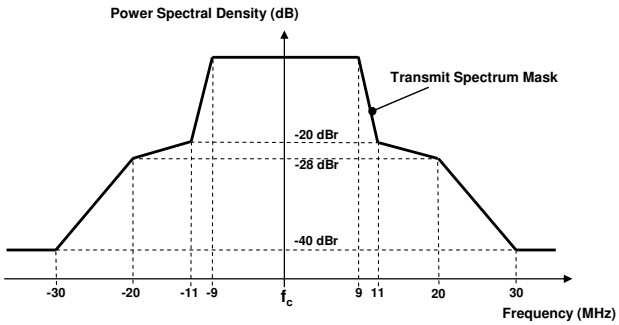

Fig. 10. IEEE 802.11a Transmit Spectrum Mask [27]

2.3. Wireless Radio Propagation Channel

The radio propagation channel distorts the transmitted signal in several ways according to the type of obstacles influencing the propagation of the electromagnetic waves [20]. First, the signal amplitude decreases due to the distance between the transmitter and receiver generally referred to as propagation loss. Second, due to static obstacles (e.g. buildings, hills and mountains) the signal amplitude is attenuated, a phenomenon known as shadowing. Finally, also time varying obstacles (e.g. moving vehicles and atmospheric variation) increase multiple propagation paths (multipath) between the transmitter and the receiver antenna.

Multipath fading affects in a different way the channel frequency bands and is thus called frequency selective fading. For a wideband signal, multipath fading acts like a random attenuation of part of the spectral components of the signal. The radio propagation between two or more antennas is statistically modeled to produce multipath effects with Rayleigh (case in which there is not any line of sight between TX and RX) and Rician (case in which a line of sight exists between TX and RX) probability distributions. Multipath presents at the receiver multiple images of the transmitted signal each of them affected by a different attenuation and propagation delay – Delay spread.

When the transmitter or/and the receiver is/are moving causes also a change in the received frequency/wavelength known as Doppler shift or Doppler effect. The Doppler shift

corresponds to a frequency variation on the signal spectrum proportional to the relative motion velocity of both TX and RX terminals.

Although, considering that the channel effects do not depend on the signal being transmitted, it tends to a linear behavior. Having in mind the propagation channel time variability, the channel is commonly assumed as a linear time-variant system (LTVS). This allows that specific blocks can be designed to effectively reverse or compensate the channel effects on the transmitted signal. In fact, the spread spectrum techniques presented on the previous section were mainly intended to generate frequency diversity to overcome frequency selective fading and also allow specific receiver architectures able to compensate propagation channel delay spreading. At the receiver module are also introduced blocks with the objective to mitigate these channel effects frequently named as channel equalizers.

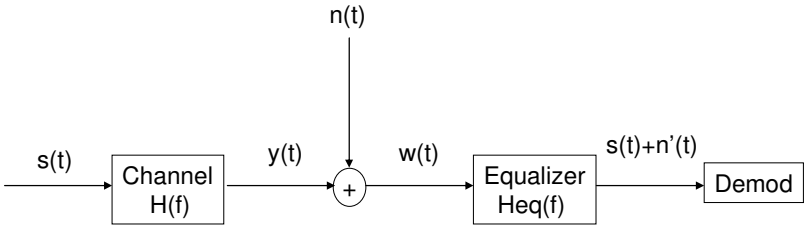

Fig. 11. Analog Equalizer Illustrating Noise Enhancement

Considering the propagation channel as a linear function, it can be represented as $H(f)$ and then the equalizer function would be ideally be $H_{eq}(f)=H(f)^{-1}$. Since the propagation channel is time variant, it is transmitted periodically a training sequence known by the receiver which gives the receiver an estimate of the channel impulse or frequency response. This will allow the receiver to track the channel response and update in real time the equalizer function parameters. The process is often referred as adaptive equalization.

Another common impairment is the near-far effect problem. This problem is referred when at one receiver the low power level coming from a far transmitter is jammed by another transmitter operating at the same band and located near the receiver. Because on the 802.11 WLAN systems under study the Carrier Sense Multiple Access with Collision Avoidance

(CSMA/CA) protocol is implemented, the near-far impact is reduced regarding that there is no channel band sharing simultaneously.

Not forgetting that the radio propagation channel can considerably distort the transmitted signal, this distortion effects are, by their nature, linear. This linearity characteristic allows the systems to functionally reproduce the inverse of the channel behavior thus overcoming the channel distortion impairments. Considering that this work is focused on nonlinear distortion impairments, attenuation was considered as the radio propagation channel in order to emulate the transmission distance.

Chapter 3

Circuit and System Simulation and Modeling

In this Chapter the platform approaches to achieve the goals of the analysis proposed for this work are described. As stated on Chapter 2, nonlinear behavior analysis requires circuit detailed nonlinear behavior representation in order to have a more realistic demonstration of the circuit response in presence of a specific signal stimulus. However, the required levels of circuit detail description is not the same for all the system blocs to achieve a good accuracy and simulation time performance.

The platform selected as the more appropriate for the study proposed was composed of a complex combination of high level abstraction (system level simulation) properly interfaced with lower level device detail (circuit level simulation). In addition, a combination of time and frequency based co-simulation algorithms was used to allow the prediction of the nonlinear component outputs in an appropriate simulation time and platform memory usage.

The Chapter starts by identifying the methodology to accurately model and simulate the nonlinear elements regarding that they are a key element for the results of this work. Secondly, the interface required to co-simulate the different levels of circuit and systems descriptions is presented. Finally, and considering the concern of the dependence of the

nonlinear output response to the signal stimulus, the platform and considerations to reproduce an exact representation of the real modulated signal are presented.

3.1. Amplifier Circuit Nonlinear Model

The main sources of nonlinear distortion on wireless radio telecom systems are the amplifiers, specially the transmitter power amplifiers as concluded at Chapter 2. This requires that these blocks need to be properly simulated to accurately predict the impact of the nonlinear behavior over the information signal. Moreover, the key nonlinear generator is actually the power amplifier active device namely the transistor. This turns it as an important piece for this study reason why special attention was paid to it.

Power Amplifier Model

To accurately reproduce the performance of the transmitter Power Amplifier (PA) it becomes necessary to carefully reproduce its behavior. A low level model detail matched with advanced simulation techniques is then required. Considering that this work focus on nonlinear analysis, an overview analysis of the PA appropriate nonlinear models and its simulation integration performance was taken for the active device model selection. Of main concern is the fact that the model shall predict with the lowest error possible nonlinear regimes and be amenable for integration into the nonlinear simulator technology elected. A circuit level representation of the Power Amplifier and the appropriate circuit design was developed to achieve the necessary performance for the systems under study.

Device Model

The active device selected to generate the Power Amplification necessary for this work was the Avago ATF-55143 Pseudomorphic High Electron Mobility Transistor (PHEMT). This device is a Gallium Arsenide (GaAs) technology transistor. The selected model for this transistor was gently provided Eng. Pedro Cabral from Instituto de Telecommunicações Pólo de Aveiro.

The active device model topology approach is a global[i] empirical circuit equivalent based model – Fager Model [22] - whose concept was developed starting from the physical device description of its nature. Its intrinsic elements behavior are empirically extracted and described by a functional description which are then defined on the platform by Symbolically Defined Device (SDD) [25] elements. Some considerations regarding the transistor model performance are stated in Chapter 4.

3.2. Amplifier Circuit Nonlinear Simulation

From the methods known [4] to accurately simulate the circuit nonlinear phenomenon, the following are highlighted:

- Harmonic Balance
- Time step integration
- Envelope Transient Harmonic Balance

Harmonic Balance Simulation

Harmonic balance (HB) is a frequency domain (Fourier series) analysis technique appropriate for the nonlinear circuits' simulation calculations. The method assumes that there is an appropriate Fourier representation of the circuit's solution when excited by a sinusoidal waveform and iteratively tries to approximate its coefficients. Being a frequency domain analysis, it is well-suited for simulating the RF systems since these are almost naturally handled in the frequency domain. The method directly captures the large signal steady state response of nonlinear systems independently from the disparity of the involved time constants and can cope with a high number of incommensurate[ii] frequencies. The steady state solution waveforms for the circuit general node voltages are approximated with a multidimensional truncated Fourier series as follows:

[i] Global in the sense that its accuracy covers a wide range of operating conditions.

[ii] Two frequencies are said to be incommensurate if their ratio is not a rational number.

(Eq.6) $$v(t) = real\left\{ \sum_{k_1=0}^{K_1} \sum_{k_2=0}^{K_2} \ldots \sum_{k_n=0}^{K_n} V_{k_1,k_2,\ldots,k_n} e^{j2\pi(k_1 f_1 + \ldots + k_n f_n)t} \right\}$$

Where *n* is the number of tones, *f1...n* are the fundamental frequencies of each source, and *K1...n* are the number of harmonics for each tone.

The circuit is represented as a system of N nonlinear ordinary differential equations, where N represents the number of circuit nodes and branch currents. The sources and the solutions are then transformed to an N*M set of nonlinear algebraic (linear) equations with unknown coefficients in frequency domain being M the total number of frequencies including the fundamentals, their harmonics and the mixing terms – the Newton-Raphson algorithm [4]. This generates, at each iteration, a matrix known as the Jacobian which is them calculated by efficient mathematical manipulations solver methods such as Krylov-subspace [24] or a direct solver.

The solver starting from an initial guess will iteratively compute the unknown coefficients until the nonlinear system of equations be satisfied within a determined maximum error from the Kirchhoff's Current Law (KCL) assumption, i.e. the KCL residual. If the method converges (that is, if the KLC residual is small enough), them the coefficients will represent the circuit steady state solution for all time.

Although HB excitation is a signal composed by multiple tones with arbitrary spacing, when increasing the number of tones the involved matrix sizes for computation increase rapidly. Analogous effect occurs when raising the input excitation power that consequently increases the number of distortion components causing higher memory and computing requirements. These factors will limit in memory and processing time which are prohibitory large for good representation of the modulated signals under study.

Time-Step Integration Simulation

The time-step integration method solves the nonlinear differential equations directly in the time domain. The method approximates the circuit's node time-domain nonlinear ordinary differential equation (ODE) derivatives by a first order finite-difference scheme.

(Eq.7) $$\frac{d}{dt}q(v(t_k)) \approx \frac{q(v(t_k)) - q(v(t_{k-1}))}{t_k - t_{k-1}}$$

(Eq.7) presents the derivative approximation by a first order finite difference formula – Backward Euler Rule.

The time step, or sampling period, between two sample instants $h=t_k-t_{k-1}$ defines the accuracy of the derivative approximation. Consequently, if the time step is smaller the number of samples becomes higher for the same signal period increasing the required processing time. The time step is commonly dynamically selected according to the signal rate of change as a compromise between accuracy and simulation time.

The time step integration method is a transient analysis method. Consequently, it should integrate over the transients until they become negligible and considered as the steady state solution. This is a problem for circuits involving too different time constants as is the case of pass band digital modulated signals. The time step method would require a huge number of simulation periods from the carrier frequency in order to achieve the steady state solution. This is often impossible to achieve on complex circuits and high carrier frequencies due to out of processing memory and excessive simulation time.

Envelope Transient Harmonic Balance Simulation

Considering that it is required to evaluate the performance of a nonlinear device operated at stronger signal levels and excited by a real modulated signal, the only actual technology capable of properly dealing with these joint requirements is Envelope Transient Harmonic Balance (ETHB). This method efficiently makes use of the best benefits of the above

referred time and frequency domain simulations techniques and properly combines its outputs. This is particularly required regarding that most communication systems transmitted signal are generated from a high frequency carrier which is them modulated by a low variation envelope having then very different time constants which in turn difficults the steady state solution estimation. Also in consideration is the fact that the carrier is by nature a periodic signal while the modulation signal (envelope) is an aperiodic signal.

ETHB is a recent research topic technique that combines the best capabilities of frequency and time domain based nonlinear simulation methods. It consists on the separation of the problem in two time scales, one at the envelope level and another at the carrier level. The information signal is represented by a time varying modulation complex envelope *A(t)* superimposing a periodic carrier f_0:

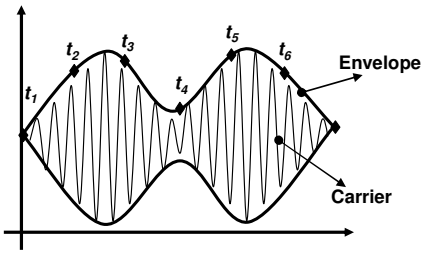

Fig. 12. Information signal representation as a carrier and an envelope

(Eq.8) $$v(t) = A(t) * e^{j 2 \pi f_o t}$$

(Eq.8) - Input information signal representation Formula

The method is based on the above described HB with the difference that on ETHB each circuit node voltage is represented by a discrete spectrum having time varying Fourier coefficients instead of a constant.

Each carrier is surrounded by a varying spectrum of +-0.5/Time step width correspondent to the bandwidth of the modulation signal. This spectrum may represent periodic signals with discrete spectral lines or also transient signals with continuous spectra which is the

case of a digital modulated carrier of the studied systems. The correspondent time domain waveform is represented as a sum of carriers where each envelope can vary with time:

$$V(t) = real\left[\sum_{k=0}^{N} V_k(t) e^{j2\pi f_k t}\right] \quad \text{(Eq.9)}$$

At each time step t_k are performed harmonic balance analyses with the amplitude and phase of the sampled envelope considering this way also the time varying envelope behavior. The method generates a sequence of spectra that characterize the response of the circuit at each t_k time instants. This would transform the problem of solving time-domain ordinary differential equation in another problem whose representation is based on differential equations to the partial derivatives in two time-domain virtual scales.

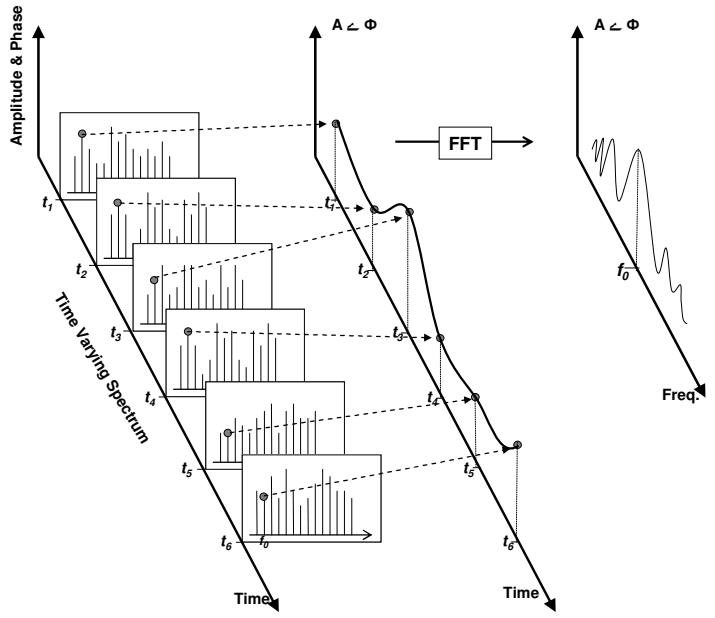

Fig. 13. Illustrative time and frequency domain process of application of the ETHB method

Nevertheless the concurrent use of harmonic balance technique on this method, the number of tones present are considerably reduced when compared to a pure multitone HB simulation. On this method, the modulation envelope can be represented using only by one tone, freeing HB tone computations for the harmonics or intermodulation products. This will avoid the matrix computation limitations from harmonic balance based algorithms.

Frequency domain models with arbitrary linear frequency response *H(jw)* can be efficiently and accurately incorporated in ETHB algorithm.

This method provides access to the instantaneous amplitude and phase modulation information for each harmonic and its spectrum by performing an FFT on its time varying value. Selecting the desired harmonic spectral line or applying FFT to the time varying spectral line possibilities all common nonlinear analyses and figures of merit.

ETHB allows I/Q baseband digital modulation to be defined by complex numerical expressions which can be generated by a numerical or Digital Signal Processing (DSP) simulation environments. This turns this method as especially suitable to interface with system level platform methodologies such as Ptolemy allowing best results predicting the device level nonlinear impairments accurately.

3.3. Simulation Platform Interfaces

With the increase of processing speed in Digital Signal Processing (DSP) circuits, a higher number of tasks on actual digital telecommunications systems are being transferred to DSP platforms. All these tasks are linearly and efficiently processed with behavioral or logical time domain signal processing models. Those behavior models were selected for the system level representation and simulation, achieving virtually the same behavior as in the real system.

A particular synchronous dataflow (SDF) computation model was firstly developed by Dennis [17] specialized on dataflow graphs where the flow control is completely predictable at compile time hence applicable to DSP systems simulation. This computation model provides the versatility and capability of predicting the behavior of any DSP based function.

Considering the fact that the mentioned telecomm systems need to be simulated in different domains at different abstraction levels, appropriate environment and interfaces

are needed. This kind of mixing and co-simulation of different environments is subject of increasing research interest. A modeling and simulator concept to deal with this environment mixture is developed under the Berkeley Ptolemy Project [5] [6].

The Ptolemy signal processing simulator concept was started at University of California at Berkeley which is now on its 3rd generation environment. The environment uses dataflow semantics with block-diagram syntax for the description of algorithms. On these environments a complex system is specified as a hierarchical composition of simpler circuits. Each sub-network is modeled by a domain that can be different from its parent. In mixing domains, the key is to ensure that at the interface, the child obeys the semantics of the parent domain.

In order to guarantee a proper interface between domains, Agilent EEsof has created a extension version of the original synchronous dataflow domain to include timed referenced components called as the Timed Synchronous Dataflow Domain (TSDF). This new domain enables the co-simulation of signal processing simulation with Envelope (ETHB) circuit simulation. The domain data type is represented by a set of five data fields namely: I, Q, Fc, time and Flavor.

$$s(t) = real\left\{\left[I(t) + j * Q(t)\right] * e^{j 2 \pi f_c t}\right\} \quad \text{(Eq.10)}$$

Where *I(t)* and *Q(t)* are the timed signal in phase and quadrature components, Fc is the carrier frequency and Flavor specifies whether the Timed data type is a carrier modulated or real-baseband format. The time step specifies the time between each sample. Thus, the sampling frequency for the envelope of a Timed arc is 1/Time step.

3.4. Signal Stimulus Generation and Detection

The generation of a random bit stream as produced by any end user wireless equipment application was considered. According to the systems studied, IEEE 802.11a and IEEE 802.11b, several digital operations are performed in order to achieve the final waveform.

Those operations accurately represent the real situation and allow the receiver model to increase the performance of the telecommunications system.

Appropriate design blocks running on a DSP platform were selected to perform the several signal operations according to the system under analysis. Those blocks/operations were Forward Error Correction (FEC), coding and decoding, interleaving/de-interleaving, mapping/de-mapping, IFFT/FFT, guard interval addition/removal, symbol wave shaping and also modulation/demodulation, up/down conversion, frequency synthesis, clock recovery, level adjustment and equalization.

Chapter 4

Platform Validation

The analysis method proposed in this work determines the design and use of component models ranging from circuit to system level detail. This Chapter summarizes the used block designs providing its characterization according to the most relevant figures of merit. It starts by presenting the main nonlinear distortion generation block that is the transmitter power amplifier and afterwards presents an overview of the excitation signal characteristics of the systems under study.

Although the two systems under study operate in different frequency bands, in this study the PA, TXs and RXs blocks were tuned to operate in the same frequency band (2.4GHz). This was assumed in order to compare the nonlinear impact on the system with different modulation and spreading methodologies maintaining the same amplifier nonlinear characteristic.

The block strategy implemented to analyze the system performance under the nonlinear impairments is presented at the end of this Chapter.

4.1. Amplifier Design

The transmit power amplifier (PA) block was considered as the nonlinear distortion generation block. The PA performance figures are shown according to the FOMs previously presented. Samples of this block were properly designed, developed and tested having as a base the nonlinear active device model presented in Chapter 4. A brief nonlinear behavior analysis of the device model used is also presented once its performance determines the system behavior.

4.1.1. Device Model

For the active device selected, there were available two models, identified as: Curtice2 – provided by the device fabricant [29] and Pedro – Developed by P. Cabral *et al.* [23]. The following pictures shown the I/V characteristic and its derivatives[i] Gm, Gm2 and Gm3 of the two device models in order to allow its performance comparison.

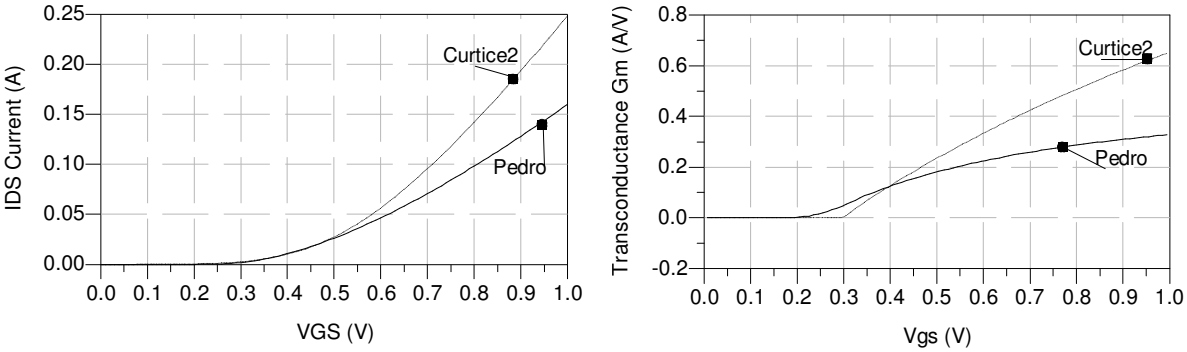

Fig. 14. Transistor drain to source current (I_{DS})(left) and transconductance (Gm) (right) curves in function of Vgs control voltage for the device models (V_{DS} = 3.5 V)

[i] $Gm_n = \frac{1}{n!}\frac{\partial^n I_{DS}}{\partial Vgs^n}$

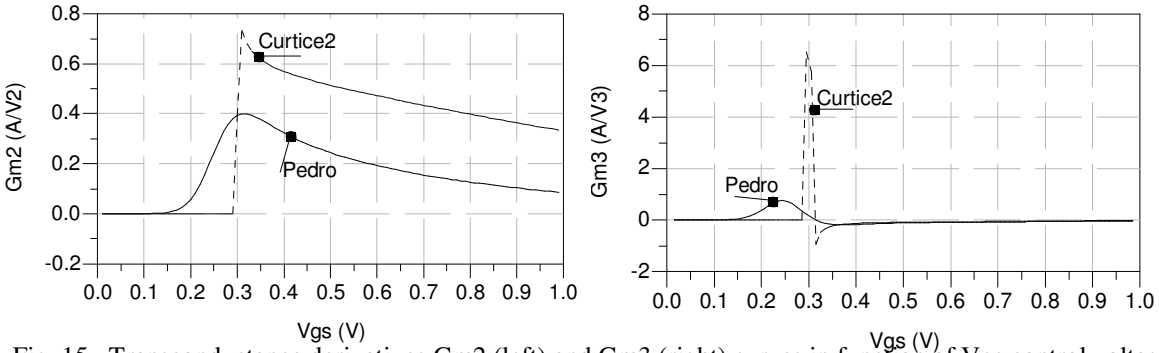

Fig. 15. Transconductance derivatives Gm2 (left) and Gm3 (right) curves in function of Vgs control voltage for the device models (V_{DS} = 3.5 V)

As the transconductance and its derivatives are determinant for the calculations of the small and large signal intermodulation distortion products, any discontinuity will difficult the simulation solution convergence. This will clearly avoid the use of Curtice2 Model for this work. The Pedro model was then selected for the studies on this work.

4.1.2. Power Amplifier

The power amplifier design targeted the achievement of similar performance than equivalent commercial equipment in terms of output power, gain and power efficiency. The circuit simplicity in terms of element reduction was also under consideration regarding the overall simulation time minimization. The design approach starts by the selection of the active device quiescent point considering device limitations and class AB operation. Afterwards, load-pull and source-pull simulations were performed in order to establish a target load and source impedances to achieve a good compromise between output power and PAE. The proper matching and bias networks were then designed to interface the established ideal impedances with the 50 ohms as in the diagram of Fig. 16.

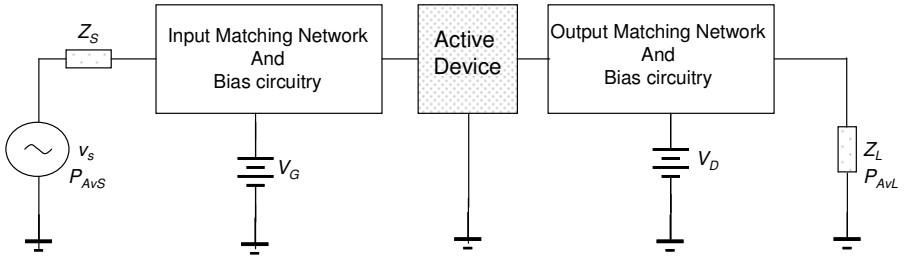

Fig. 16. Functional diagram of the PA model

A first PA design (Fig. 17) use distributed microstrip network lines for impedance matching and proper bias to guarantee the operation in class AB.

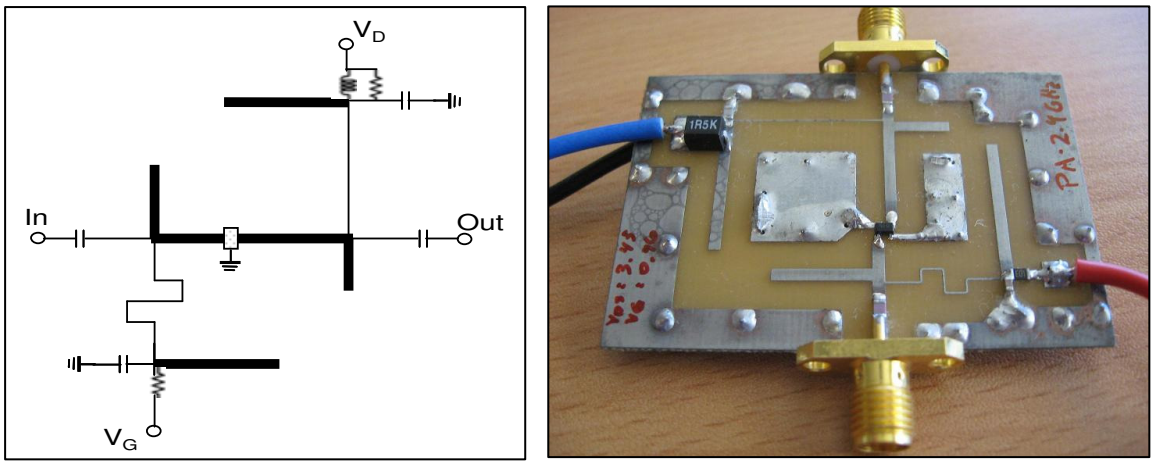

Fig. 17. First PA design circuit schematic (left) and picture of an implemented test board (right)

A second PA design was also considered as a straightforward circuit version. In addition to the proper bias DC sources (using inductor chokes for RF isolation), this second circuit consists on the direct application of the 50 ohms load impedances to the device gate and drain ports. Fig. 18 shows the AM/AM and AM/PM characteristics of the above-referred PA first design (Complete Model) as well as the second design with the simplified matching and bias networks (Simplified Model).

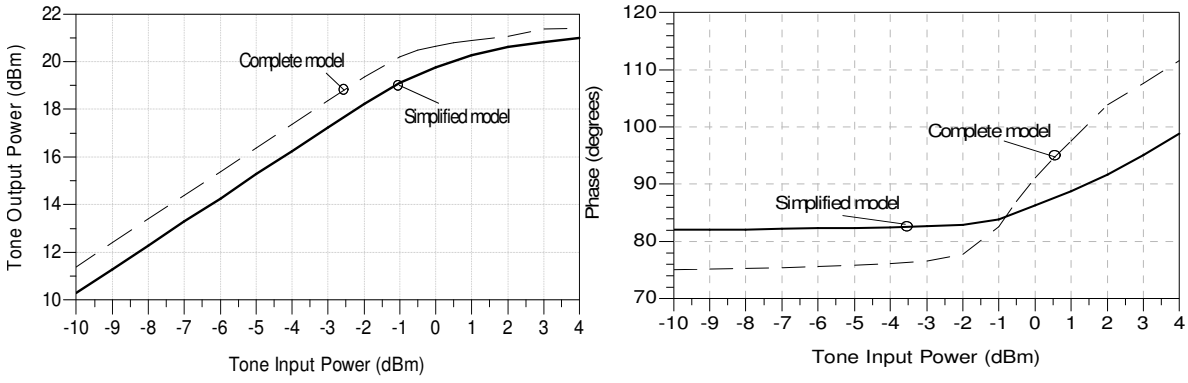

Fig. 18. AM/AM (left) and AM/PM (right) power amplifiers simulated characteristics

As can be observed from Fig. 18, the Complete Model presents a P1dB of around 20,5dBm and the Simplified Model presents a P1dB of around 21dBm. The Complete Model and the Simplified Model presented a PAE of 45% and 39%, respectively (for 0dBm of input power). Additionally, a slightly higher power gain can also be noticed for the Complete

Model. From the system-level behavior point of view, both characteristics can be representative of a real power amplifier system.

The not use of matching networks on the Simplified Model will also reduce performance in terms of amplifier matching. From a system level perspective, and for the platforms under consideration, the input and output PA mismatching do not influence the overall system simulation results. The PA model block does not electrically load the adjacent system level blocks under any circumstance on the developed platforms. Having in consideration the simulation time reduction for the system level platforms and the similar model performance, the Simplified Model was selected for this study. The PA Simplified Model will be onwards considered as the power amplifier. On the following pages are presented the main nonlinear performance characteristics from the adopted PA Simplified Model.

Fig. 19 visualizes the output of the one-tone excitation. As can be seen, the nonlinear harmonic generation is under 39dBc for the 0dBm input power level.

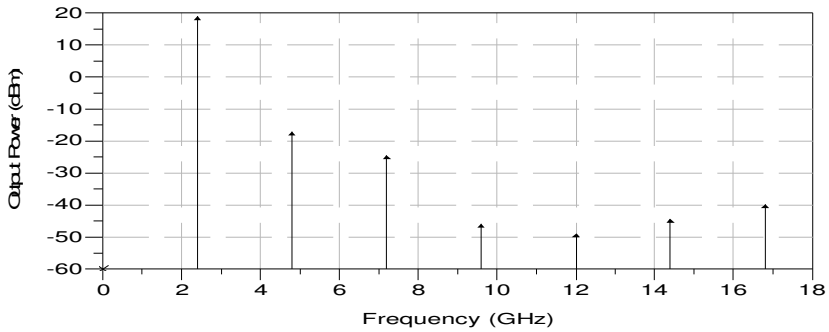

Fig. 19. Simulated one tone nonlinear harmonic generation for 0dBm tone excitation power

Regarding odd order intermodulation distortion, the major impacting orders as the 3rd and 5th are stated on Fig. 20 as a function of the output power levels for two tone products. The 5th order products are around 10dB under the 3rd order levels for the considered PA operation output power range turning they as practically shaded by the 3rd order effects.

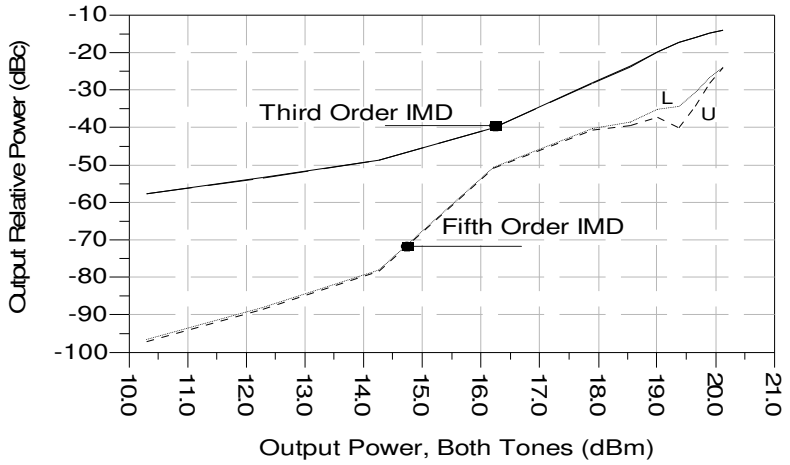

Fig. 20. Power amplifier simulated 3rd and 5th order intermodulation behavior (upper and lower bands)

As expected, the higher PA power added efficiency (PAE) values are reached for higher saturation regimes with, consequently, reduced Transducer Power Gain as on Fig. 21. The designed amplifier operates with PAE ranging from 20% to 40%. Slightly higher PAE values could be achieved at the cost of higher design complexity, which as a result would increase the required simulation time.

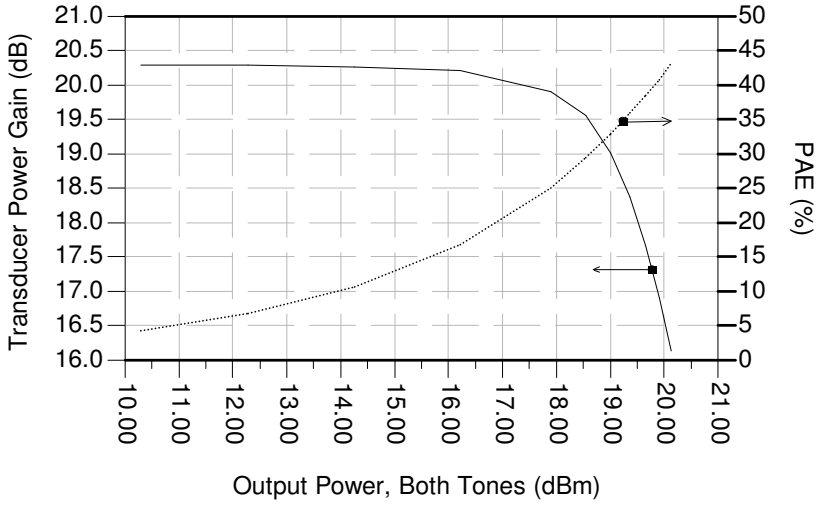

Fig. 21. PA simulated PAE and transducer power gain as a function of output power (two tones simulation)

4.2. Signal Excitation Characterization

For the signal excitation generation was selected a system level design, to be simulated with Timed Dataflow [28], together with Ptolemy [5][6] simulation strategy. Considering that the instantaneous signal power level determines the nonlinear effects, a brief characterization of the waveform shapes and their stochastic nature are presented.

4.2.1. DQPSK/CCK Modulated IEEE 802.11b

As mentioned above, for the analysis of a CCK signal, the IEEE802.11b excitation was used with the standard maximum allowed data rate of 11Mbps. The signal constellation and sample envelope waveform is as shown on Fig. 22 and Fig. 23, respectively.

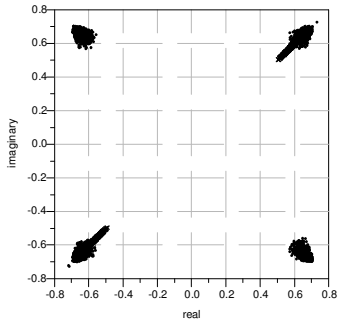

Fig. 22. DQPSK I/Q Signal constellation of the IEEE802.11b at 11Mbps data rate

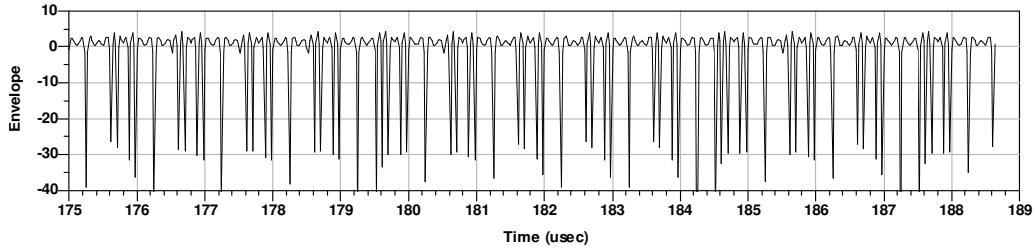

Fig. 23. Sample detail envelope waveform of the transmit data IEEE802.11b burst of 11Mbps data rate

In the previous signal waveforms it can be verified that the 802.11b signal presents an unambiguous average level. The average level referred is not affected by high positive variations but only negative variations. This fact can be better illustrated by its statistical

behavior namely its Complementary Cumulative Distribution Function (CCDF) as shown in Fig. 24.

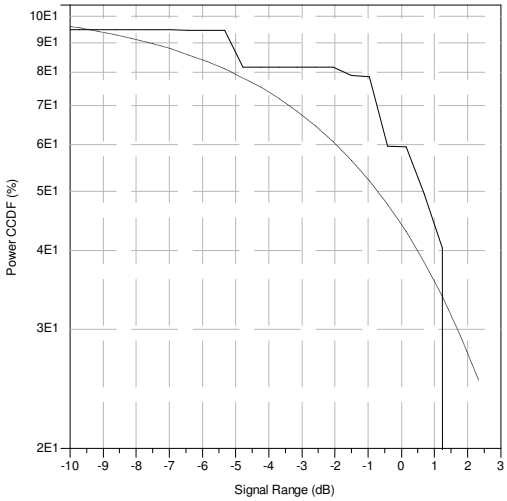

Fig. 24. Relative power complementary cumulative distribution function of the 802.11b signal waveform (solid) and the distribution of an Gaussian signal (dashed)

After statistical processing of the measured signal, the CCDF curve provides an estimate of the probability of the signal being at or above a given power level, expressed in dB relative to the average power. The CCDF of the 802.11b signal confirms the lower probability of higher power increases. This fact will limit and minimize the nonlinear products generated when applying this waveform to a nonlinear device on a signal transmission chain.

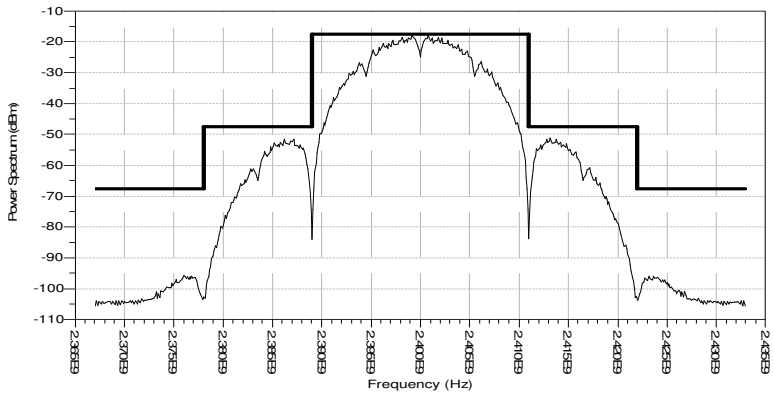

Fig. 25. Power spectrum example of an IEEE802.11b signal and the IEEE Std 802.11b-1999 section 18.4.7.3 specification spectrum mask (bold)

Fig. 25 shows an example of the power spectrum and correspondent standard mask from an 802.11b signal with Gaussian type output shaping filter.

4.2.2. M-QAM/OFDM Modulated IEEE 802.11a

For the analysis of an OFDM signal, the IEEE802.11a waveform was considered with the options of maximum data rate of 54Mbps and the QPSK mode with 18 Mbps data rate for comparison with the 802.11b signal characteristics.

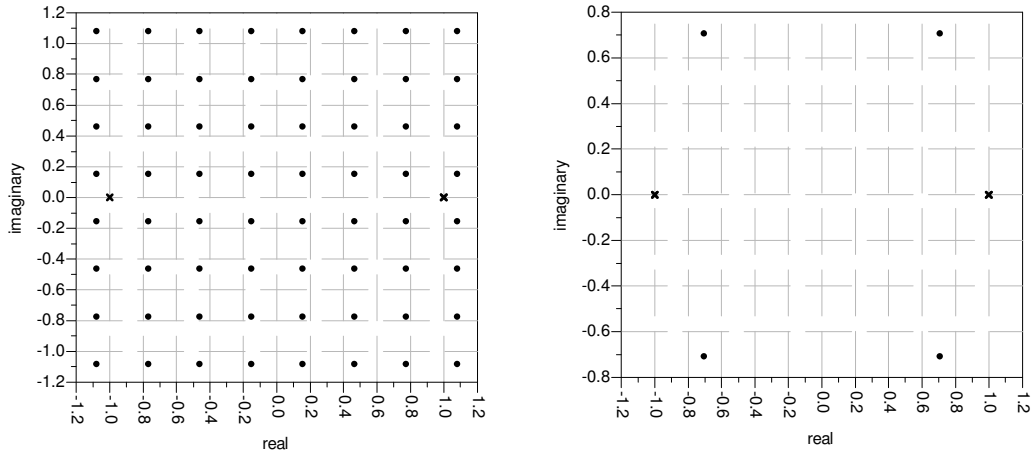

Fig. 26. IEEE802.11a signal IQ constellations for the mode of 54Mbps 64-QAM (left) and 18 Mbps QPSK (right)

As described on Section 2.2.2, the 802.11a 54Mbps mode is modulated on a 64-QAM IQ constellation levels and the 18 Mbps mode is modulated on a QPSK IQ constellation shown on Fig. 26. On the next figures are presented samples of the 802.11a envelope waveform and a close up view from the waveform sample.

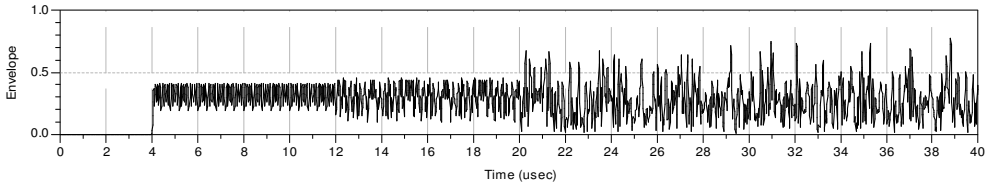

Fig. 27. Envelope waveform of the IEEE802.11a burst

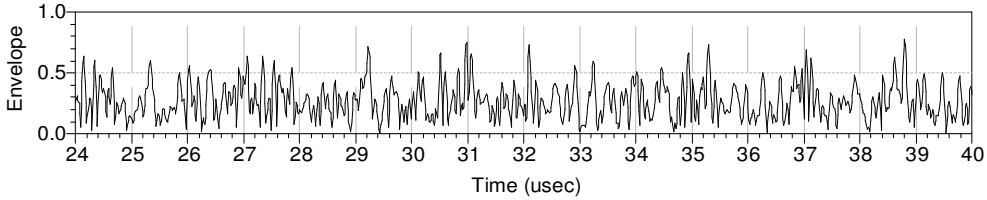

Fig. 28. Envelope waveform detail of the data field of an IEEE802.11a burst

In contrast with waveform from the 802.11b modulation, the visual inspection evidently shows that this waveform presents a permanent high variation range levels. This fact is confirmed by its statistical cumulative distribution shown on Fig. 29.

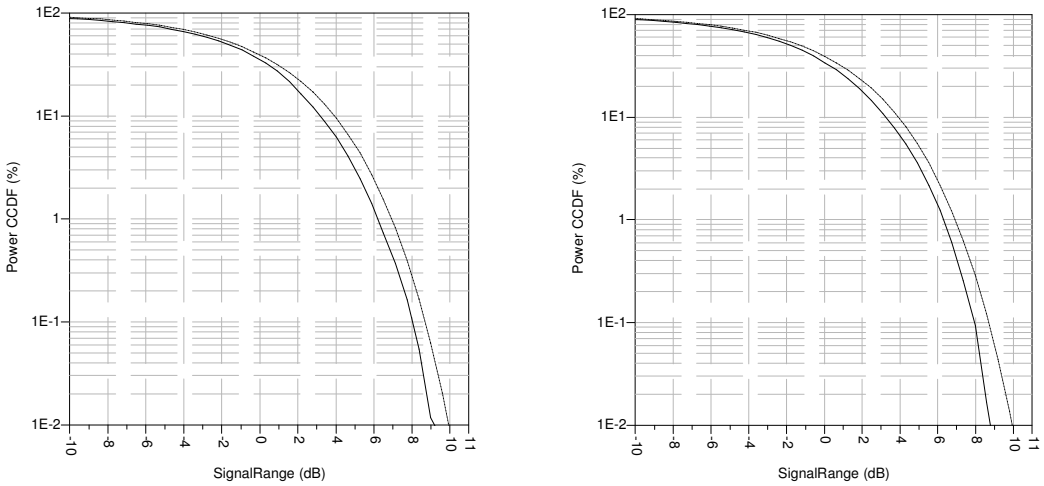

Fig. 29. Power complementary cumulative distribution functions of the 802.11a signal waveform and the distribution of an Gaussian signal (-). At mode 54 Mbps (left); at mode 18 Mbps (right)

The CCDF of the 802.11a waveform resembles to the distribution of a Gaussian noise source within a bandwidth. The Fig. 30 shows the spectrum of an 802.11a signal and the correspondent IEEE Standard spectrum mask.

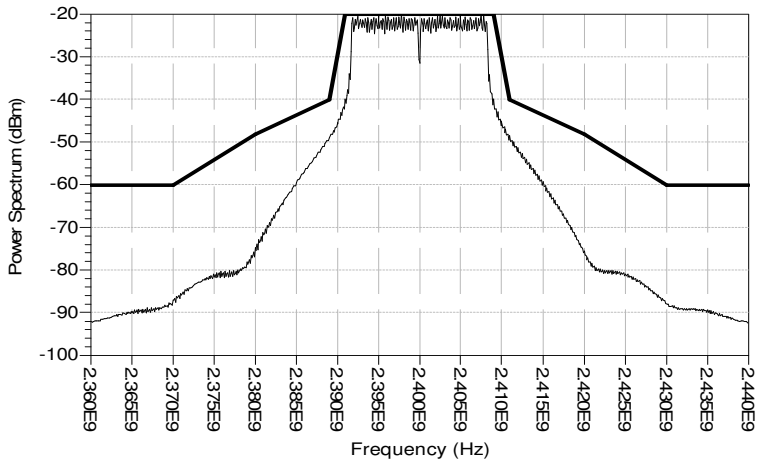

Fig. 30. Power spectrum example of an IEEE802.11a signal and the IEEE Std 802.11a-1999 section 17.3.9.2 specification spectrum mask (bold)

4.3. Platform interfaces and system level analysis

A system level approach was considered in order to analyze the performance of the systems under evaluation when affected by nonlinear impairments. A block diagram of the approach is presented on Fig. 31.

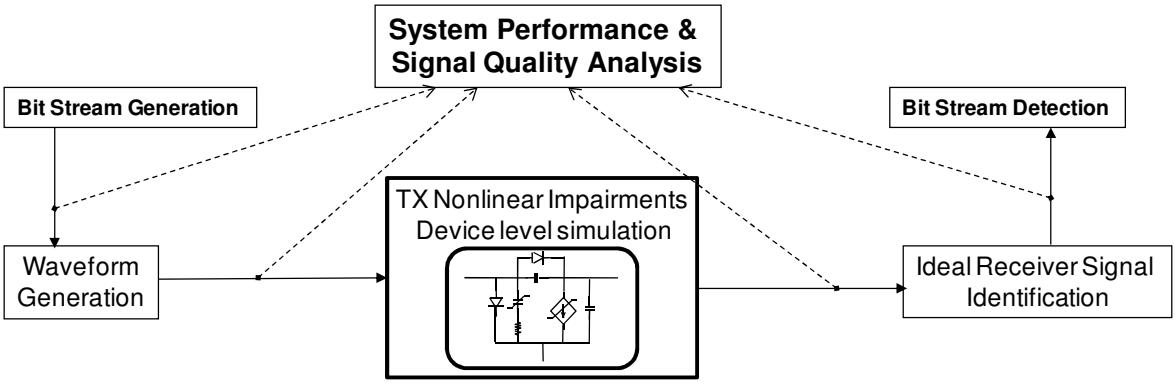

Fig. 31. Implemented wireless test bench, system level block diagram (functional)

The waveform quality is followed on its different blocks and a signal quality inspection is performed according to its modulation constellation and also an end-to-end approach as bit error counting.

Error Vector Magnitude

The Error Vector Magnitude (EVM) figure of merit is a direct measure of modulation accuracy and transmitter performance. The difference between a measured signal and its ideal error-free point in the constellation is defined as the error vector, as shown in the complex plane in Fig. 32.

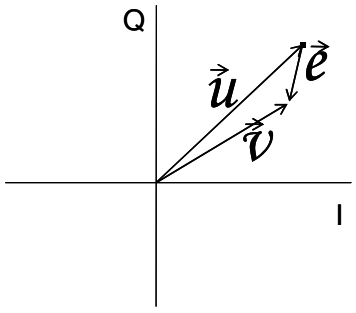

Fig. 32. Modulation constellation vector representation on complex I/Q plane

EVM is a statistical estimate of the magnitude of the error vector normalized by the magnitude of the ideal signal. For a specific symbol, EVM is mathematically defined as (Eq.11).

$$EVM = \sqrt{\left[\frac{\sum_{K=1}^{M} \left\| \vec{v}(k) - \vec{u}(k) \right\|^2}{\sum_{k=1}^{M} \left\| \vec{u}(k) \right\|^2} \right]} \quad \text{(Eq.11)}$$

Where $\vec{v}$ the measured signal; $\vec{u}$ is the ideal modulated signal; M is the number of measurement samples; and k is the sample index. Equation (Eq.12) presents the EVM conversion to dB values.

$$EVM_{dB} = 20 * \log_{10}(EVM) \quad \text{(Eq.12)}$$

Bit Error Rate

Another system quality analysis is the bit error counting from signal path end to end. The bit error rate (BER) is the most common quality figure of merit of a telecommunications system. Other figures of merit such as packet error rate (PAR) or frame error rate (FER) are also common. The latter were defined considering that the mentioned systems operate with digital error correction schemes such as forward error correction (FEC) which have the capacity to recover a determined number of errors with the cost of the addition of redundant bits.

$$BER = \frac{NErrors}{Nbits} \quad \text{(Eq.13)}$$

Although being a good system level figure of merit, the BER has some drawbacks when using it [21]. The method needs information from the complete operation of the telecommunications system under study to enable the bit comparison from transmitter input to receiver output. In general, BER analysis requires considerable high amounts of test transmitted bits in order to have statistical validity confidence. The proposed BER simulations on this work mainly focus on the quality degradation analysis so reducing to a minimum the amount of transmitted bits that allow a valid overview of system performance degradation.

Chapter 5

System Nonlinear Impact

After presenting the characterization of the phenomenon object of this study and the tools to perform the appropriate analysis on the systems under consideration, this Chapter presents individual case studies focusing different impairments caused by the nonlinear phenomenon.

In the first two sections are presented the measurements of the impact of the nonlinear distortion generated by the power amplifier on the systems under study. This analysis allows the quantification of the distortion introduced by the phenomenon as a function of the input PA excitation power applied.

In a second stage, at Section 5.3, the odd order intermodulation distortion impact on adjacent spectrum is evaluated for the herein presented OFDM system. The analysis allows a quick evaluation of the system performance degradation as function of the introduced nonlinear generated power by an interfering nonlinear adjacent system.

5.1. Signal Degradation Analysis on CCK Systems Due to Nonlinear Distortion

This study analyses the signal quality degradation when affected by nonlinear distortion effects, a phenomenon that in this study case is concentrated uniquely on the transmitter

power amplifier. The figures of merit used for these analyses were presented on the previous chapters. For this study, the signal excitation and power amplifier characterizations were presented on Chapter 4.

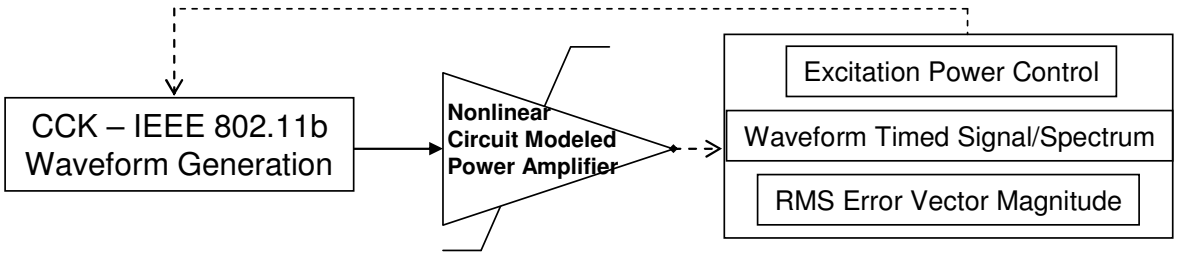

Fig. 33. High-level block diagram of the analysis performed for a CCK system

The platform setup for this analysis consists on the injection of an 802.11b waveform on the power amplifier described on Chapter 4. The output from the power amplifier is then processed and compared against the original excitation signal in order to assess impact analyses.

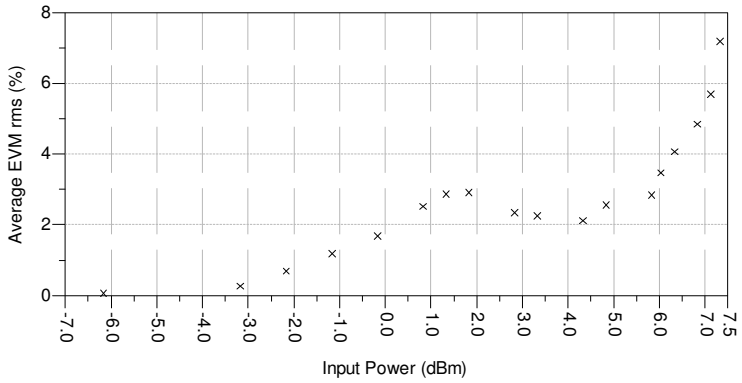

Fig. 34. Error Vector Magnitude behavior versus power amplifier input power

Being the 802.11b a DQPSK based modulation it has a high margin for constellation error and, in consequence, it is not standard limited by EVM values but only by adjacent spectrum power.

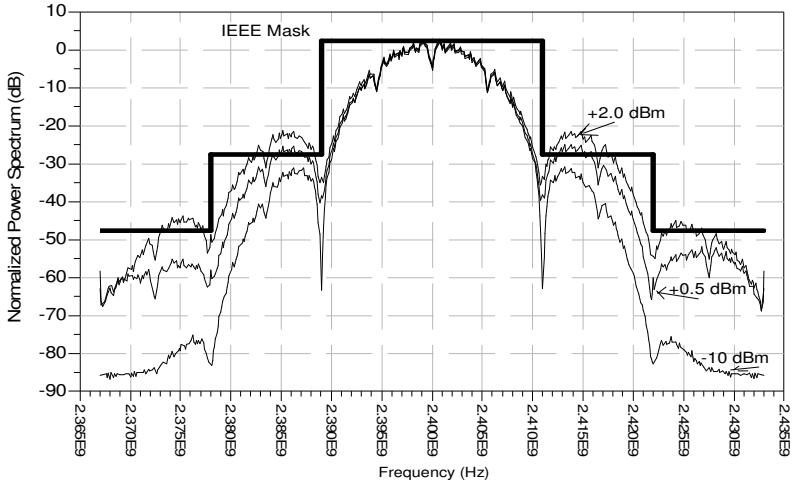

Fig. 35. CCK PA output normalized power spectrum for -10dBm, 5dBm and 2dBm input excitation levels

As can be verified on Fig. 35, the power amplifier under test cannot be excited with more than 0.2dBm in order to comply with IEEE standard spectrum mask. For higher power values, the nonlinear generated spectral regrowth exceeds the allowed power margins and increases the impact on adjacent channel systems.

5.2. Signal Degradation Analysis on OFDM Systems Due to Nonlinear Distortion

Following the previous analysis of a CCK modulation, this section concentrates on OFDM modulated systems. This analyzes the signal quality degradation when affected by the nonlinear distortion effect. The figures of merit used for these analyses were presented on the previous chapters. For this study, the signal excitation was presented on Section 4.2.2.

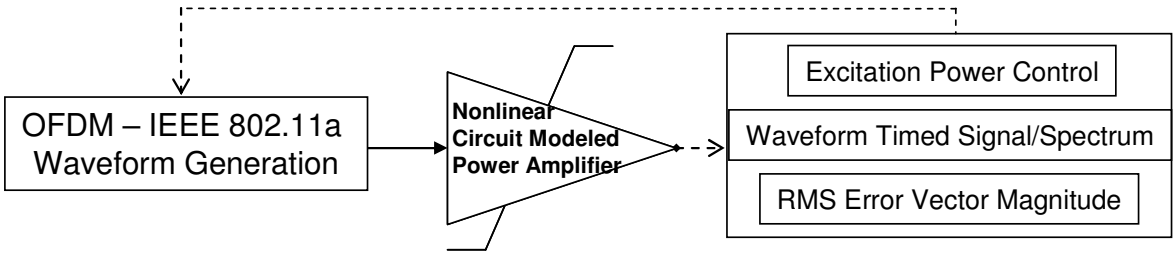

Fig. 36. High-level block diagram of the analysis performed for a OFDM system

The platform setup for this analysis consists on the injection of an 802.11b waveform on the power amplifier described on Chapter 4. The output from the power amplifier is then

processed and compared against the original excitation signal in order to assess impact analysis.

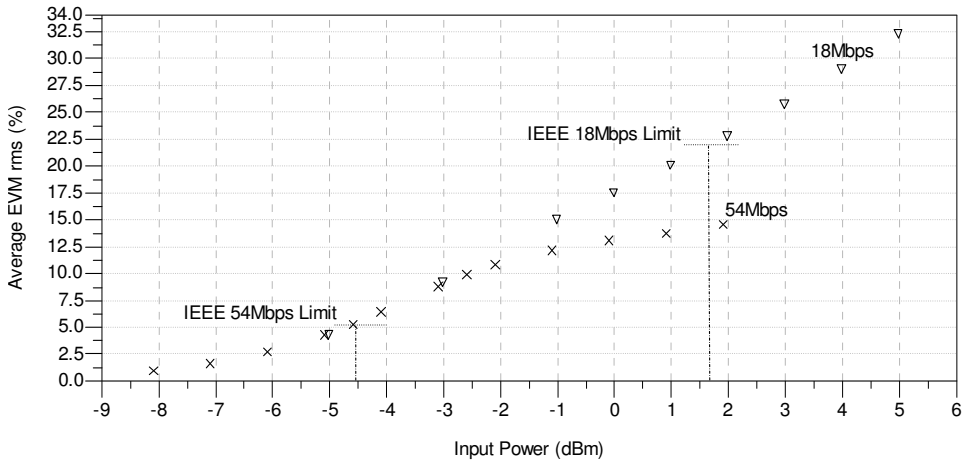

Fig. 37. Average error vector[i] magnitude versus power amplifier input power for two different data rate

The higher IQ constellation density from 64-QAM modulation format has a reduced error margin, i.e., it has a lower margin for signal nonlinear distortion effects. As can be verified from Fig. 37, the 54Mbps signal is limited by its maximum allowed EVM by the maximum PA input power of only about -4.5dBm. With higher error margins, the 18Mbps rate would allow up to 1.7dBm of PA input power.

In opposition to the herein analyzed homologous 802.11b system, the 802.11a standard power spectrum mask has considerable margin to increase adjacent spectrum distortion level when operated at higher data rates such as 54Mbps. In the Fig. 38 it can be verified the maximum PA input power limitation being of around 1.5dBm for the 54Mbps data rate.

[i] EVM calculation was done according to IEEE 802.11a -1999 standard, i.e., sampling the signal over all the OFDM data subcarriers that constitute a symbol and over all the OFDM symbols that constitute a frame then normalizing by the average power of the signal constellation and averaging over at least 20 frames.

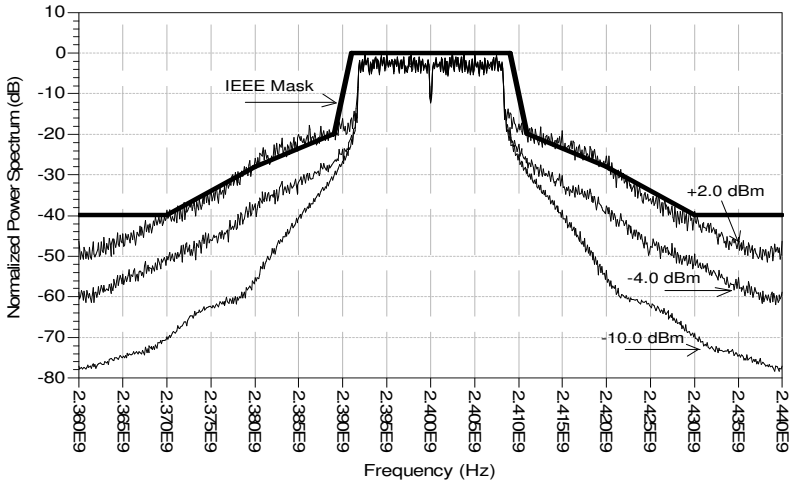

Fig. 38. OFDM normalized output power spectrum comparison with IEEE spectrum power mask

5.3. Odd Order Intermodulation Distortion Impact on Adjacent Spectrum

The impact of the nonlinear distortion on adjacent channels and on adjacent systems is the main concern of regulation authorities. This results on a set of regulations created to limit the maximum allowed power generated on other bands than the one in use. These regulations directly determine the admissible nonlinear system performance, and consequently systems' output power amplifiers.

In this case study, the performance impact on an ideal transmit/receive setup is analyzed when affected by the odd order nonlinear distortion generated by an adjacent band system. The following Fig. 39 illustrates the spectrum perspective for the variations under analysis.

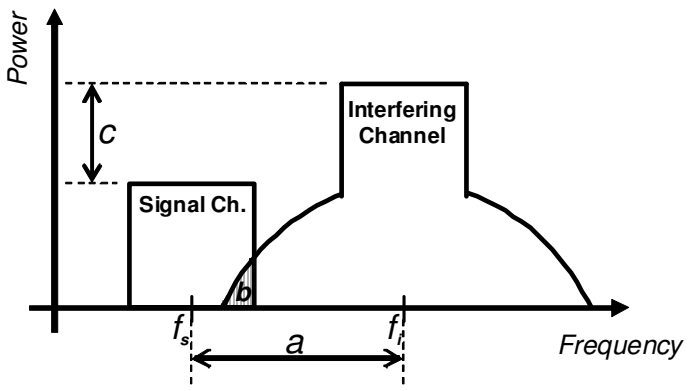

Fig. 39. Spectral illustrative view of the variations under analysis

The three variation degrees studied are illustrated on Fig. 39 and identified as ***a***, ***b*** and ***c***. The ***a*** variation corresponds to the carrier frequency separation of the adjacent systems under study. The closer the system can operate the higher global spectrum efficiency is achievable. In opposition, the lower frequency separation, the lower relative operational dynamic range of the all system is supported. The shaded area, identified as ***b***, corresponds to the amount of nonlinear generated interference noise superimposed into the ideal transmitted signal. This quantity is directly linked to the nonlinear odd order distortion products generated by the interferer system and so directly dependant on its power amplifier excitation saturation level. The ***c*** variation corresponds to the relative power difference between the two systems. The relative power can simulate for example the distance difference between the two systems and the receiver. The more distant a system is, the lower power reaches its receiver and then more susceptible it is to any interference such as adjacent channel nonlinear distortion products. This effect corresponds to the so-called "near-far effect" considering that the two systems are tested with concurrent bursts.

Platform design considerations:

Any digital signal is, by its nature, time sampled. Any digital operation or process requires fixed instant selection to be performed. In summary, all digital operations require a time step to rule its cadency and consequently its synchronization. This fact concludes that all digitally simulated components will be correlated by its time step inter operation cadency.

In order to proper study two different systems concurrently operated, a first consideration is that they must to be uncorrelated to achieve realistic results. The approach to overcome the time step correlation problem was to use a high degree of oversampling in relation to the single bit time, together with the complex modulation operations and the large number of different samples. This way, the results would converge to the correct statistical final value. These considerations may be visualized on the signal samples shown in the following figures. Fig. 40 shows a sample of the two waveforms produced by the signal and interferer systems just before being modulated and converted to the respective carrier frequencies by the IQ modulator.

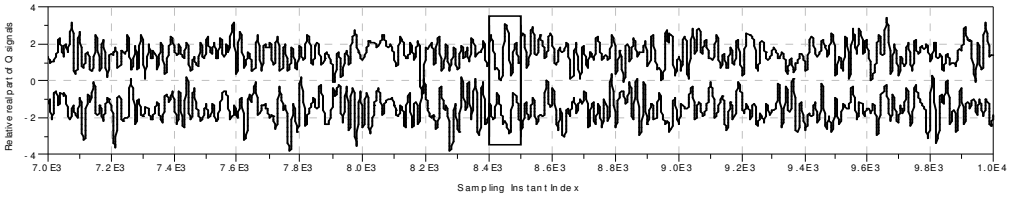

Fig. 40. Detail of the Q signal waveform of the data field of both signal and interferer generators

Fig. 41 zooms into detail the Q sample of the waveform generated by the signal and interferer, with evidence to the high oversampling used in order to avoid impact from correlation due to time step and digitalization of both signals.

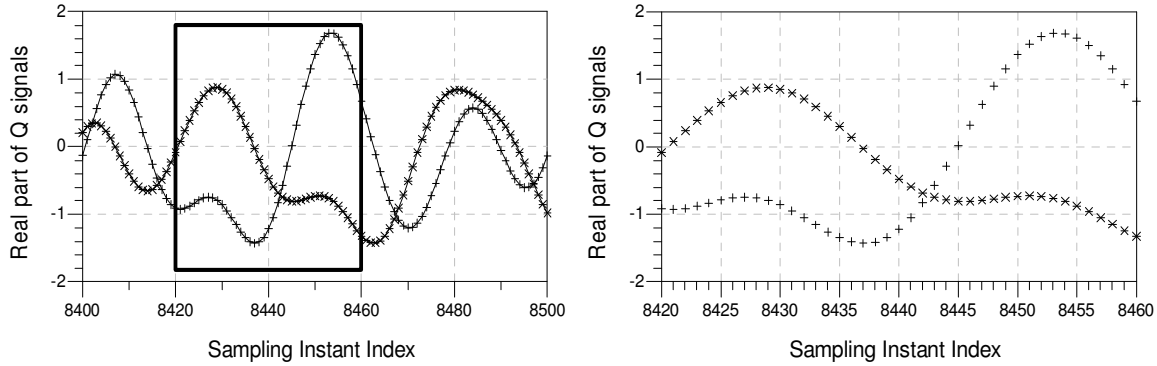

Fig. 41. Sampling instants detail of 100 samples view (left) and 60 samples view (right)

Additionally, to increase the closeness to reality, both systems were configured with different bitrates, with a slightly delay between the start transmitting moment and also with different scramble codes. This guarantees that both systems would virtually transmit different signals from both systems and minimizing the impact of correlation imposed by the digital sampling instant.

The addition of the two signals needs to be carefully prepared in order to properly synchronize both applied signals before entering the sum block. This is considering that the two systems operate in different sample rates so filtering and time step synchronization are then required.

A signal-conditioning block comprises the necessary operations to isolate the band of interest to be properly detected by the receiver. These operations are namely the

redefinition of signal carrier frequency, sampling frequency conversion and finally ideal filtering/selection the band of interest.

The receiver module has carrier synchronization and adaptative filtering operators to properly decode the data bits. The output data bits are compared with the transmitted bits by the BER block in order to count the total number of errors occurred.

Both terminals were configured to have a small delay between their burst start moment, although, the data transmission fields are completely time superimposed. Each data burst contains 1000 information octets, being sent a minimum of 25 bursts per BER point simulation. The first burst was not considered for the bit error count.

As referred on previous section, this study does not intend to deeply quantify the quality of the systems but actually qualitatively evaluate the system behavior when affected by interference generated by the nonlinear distortion phenomenon.

The nonlinear interference, Gaussian noise and system power was calculated by integrating the spectrum energy over the bandwidth under consideration. The used 802.11a signal has 16.6MHz off occupied spectrum bandwidth.

Platform setup description:

The signal flow starts from two separate similar ideal IEEE 802.11a WLAN systems modulating different bit sequences. One of the systems, onwards called as interferer, the nonlinear PA referred on Chapter 4. amplifies the signal generating nonlinear spectral regrowth products. Both signals are synchronously added and conditioned in order to select the appropriate band for the receiver. Following the Fig. 42 shows the diagram of the platform setup considered.

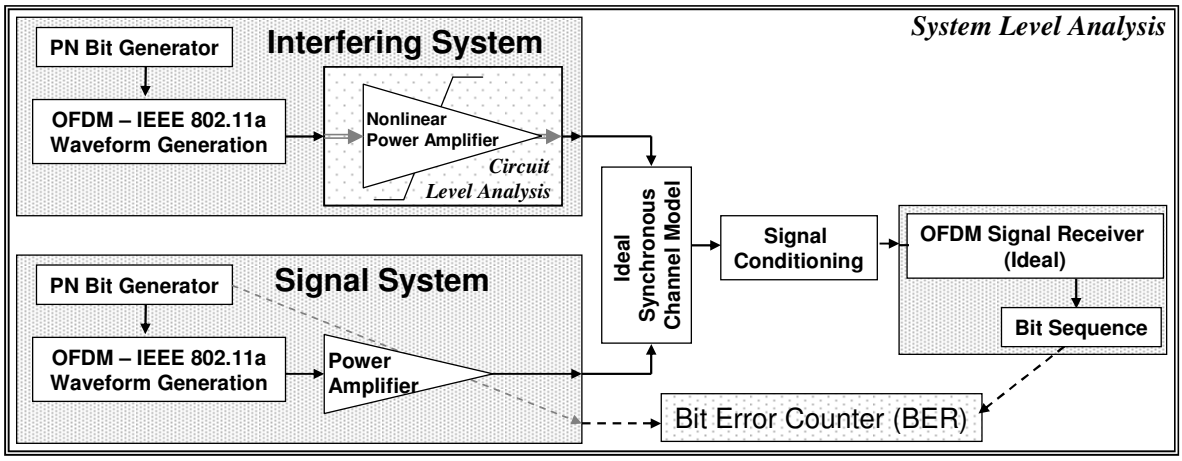

Fig. 42. Adjacent channel nonlinear impact analysis functional block diagram

The next set of Fig. 43 to Fig. 45 shows examples of different operation conditions on different measurement points over the platform. On Fig. 43 can be visualized the effect of the nonlinear power amplifier on the signal waveform. This block used ETHB type simulation as referred on Section 3.2.

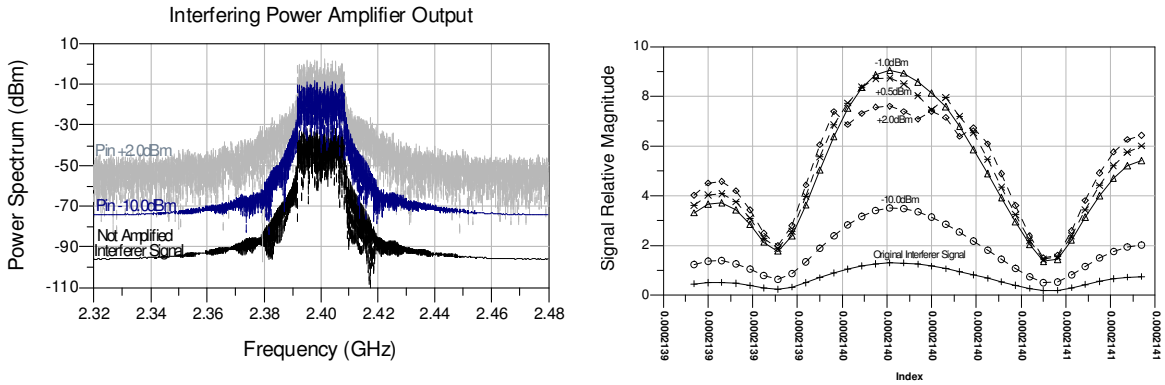

Fig. 43. Output spectrum (left) and magnitude (right) of the interferer's NL power amplifier

On the next figures, are presented two power spectrum extreme examples measured at the correspondent output of Signal and Interferer systems. The two test cases presented on Fig. 44 correspond to the minimum (16 MHz) and maximum (26 MHz) carrier frequency separation with different excitation power configurations.

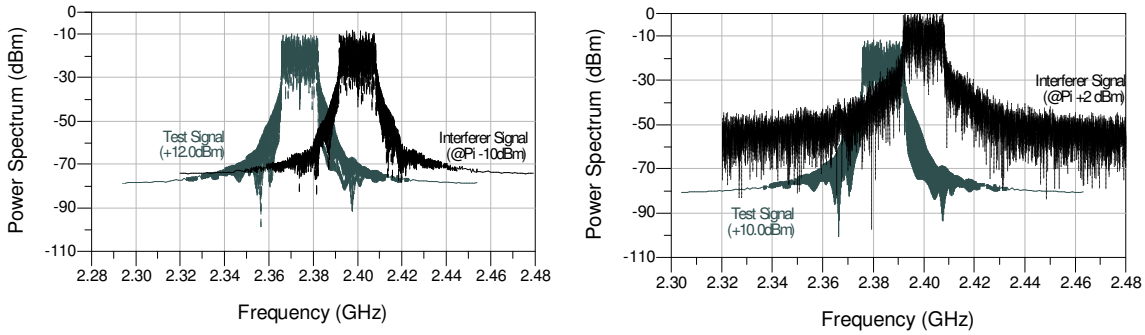

Fig. 44. Spectrum visualization example of the interferer and test signals for two test cases

Fig. 45 depicts an example case of the spectrum at the propagation channel.

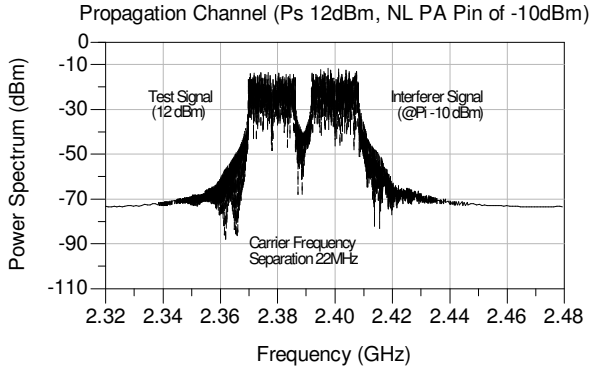

Fig. 45. Example of the spectrum at the propagation channel for a test case

In addition to the above-referred platform, a similar platform was considered replacing the nonlinear interferer by a white Gaussian noise generator in order to enable the comparison of the impact of the two types of interfering sources. The white Gaussian noise power values presented were calculated by the integration of the correspondent instantaneous energy along the bandwidth under consideration. The following figures show the summary of all the study case combinations in terms of interfering signal power.

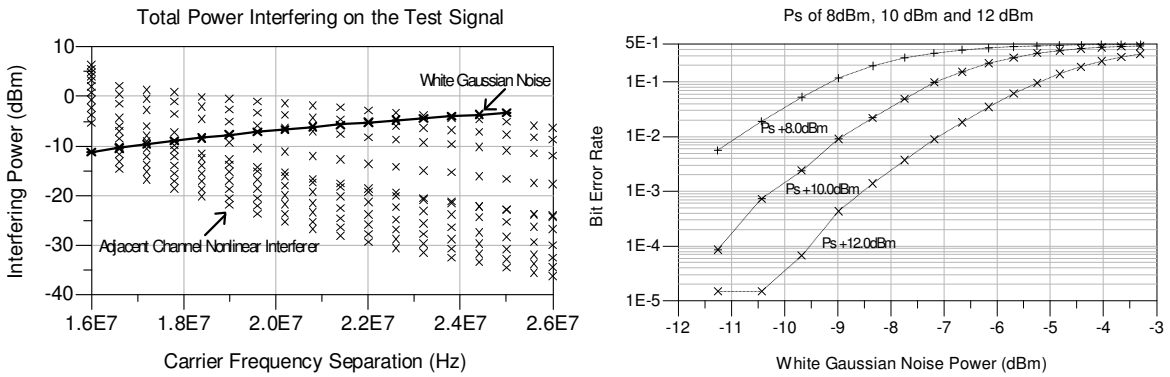

Fig. 46. Summary visualization of all the test cases in terms of interfering power applied: nonlinear adjacent channel (left) and Gaussian noise (right)

BER simulation outputs:

The following set of figures (Fig. 47) shows the BER results for the different variation cases above discussed. The system behavior can be analyzed as a function of the interfering carrier proximity for different values of signal excitations. The plots show the consequent increase of error bits when the received power from the interferer is increased.

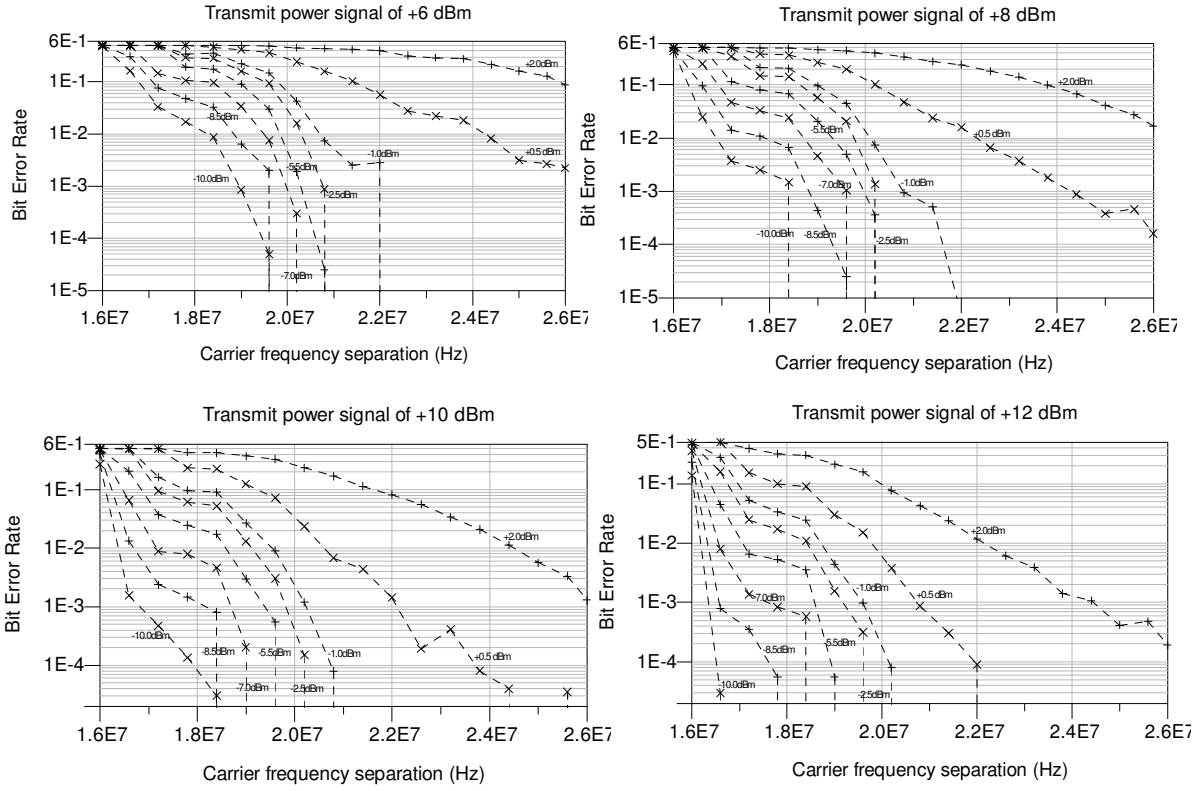

Fig. 47. BER statistics as a function of the carrier frequency separation for different signal and interfering power levels

In Fig. 48 are compared different transmitted power applied to the signal, here it is observable the consequent increase of error bits when reducing the signal power. This reduction corresponds to the reduction of the signal to noise ratio. These results can be useful to evaluate a possible real time decrease of channel frequency separation allowing the total bandwidth efficiency increase.

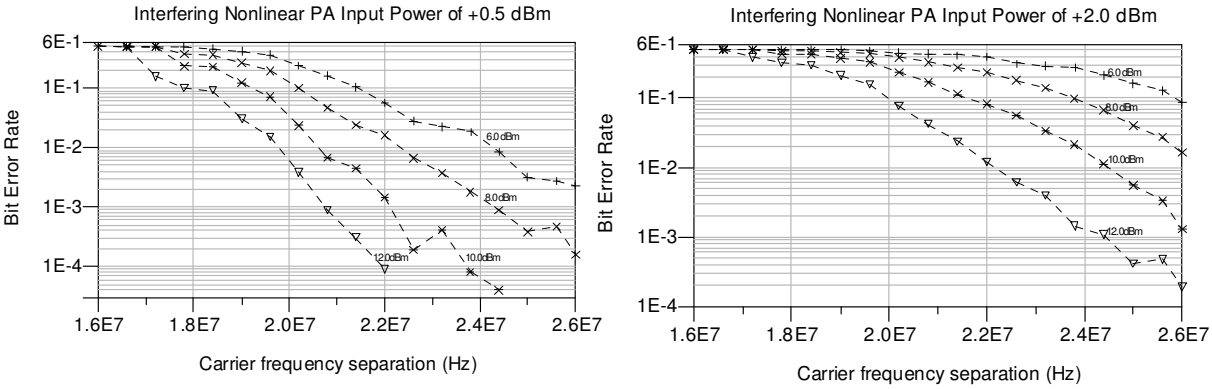

Fig. 48. Comparison of BER statistics as a function of the carrier frequency separation for different signal power levels for interfering PA excitation levels of 0.5dBm (left) and 2.0dBm (right)

By integration of the power that is affecting the test channel (signal), the following set of figures (Fig. 49) compares the white Gaussian noise with the noise generated by the uncorrelated nonlinear adjacent channel source (considering the same total interfering power). It can be verified a higher impact of the nonlinear noise than the white Gaussian noise.

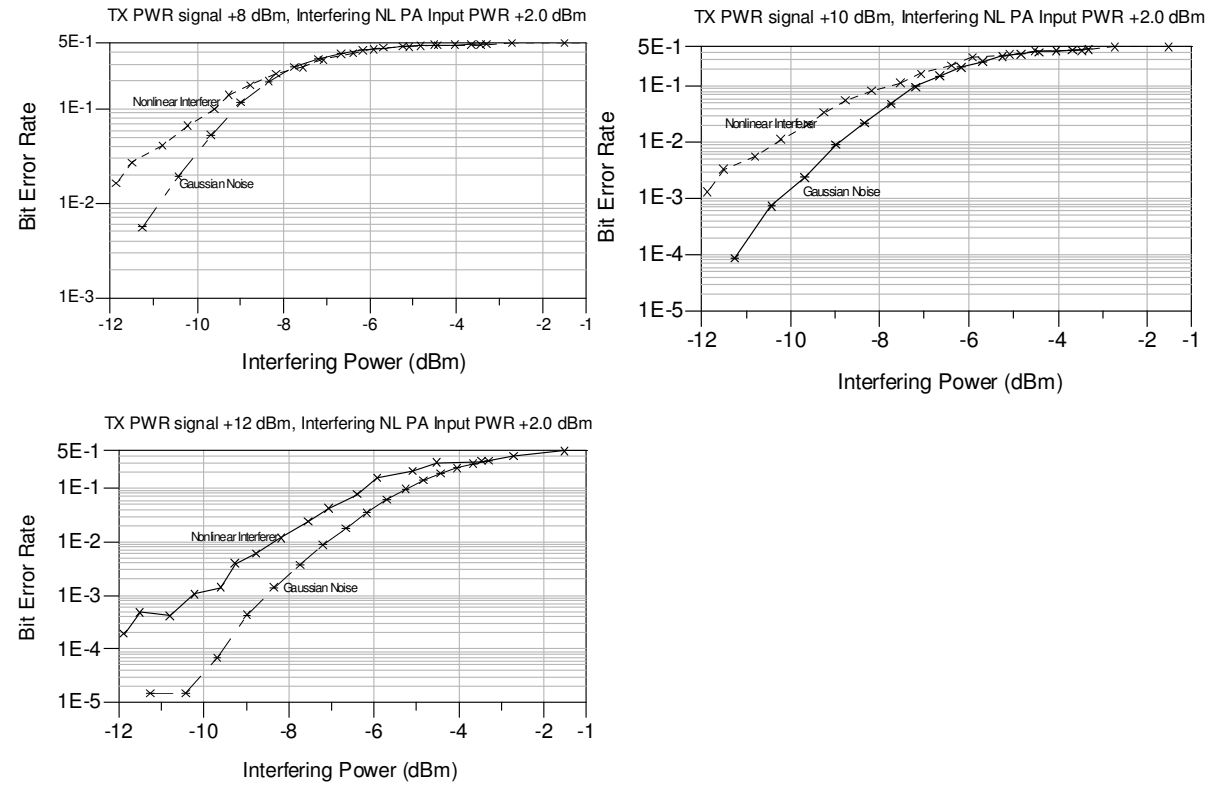

Fig. 49. Comparison of BER statistics as a function of the total interfering power (Gaussian noise and NL generated noise) for different levels of signal power, Ps of +8dBm (up left), PS of 10dBm (up right) and Ps of 12dBm (down left)

In the following set of plots (Fig. 50) it can be analyzed the different impact according to the different levels of saturation of the nonlinear power amplifier. This study is carry out by the excitation of the nonlinear PA with different power levels and then measure the total power impacting on the signal under test. Those measurements present a non-monotonous performance along different interfering power if generated by nonlinear source in opposition to the white Gaussian noise behavior. Another aspect is that the higher level of saturation of the interfering PA output the lower impact on adjacent signal (considering the affectation of the same total interfering power).

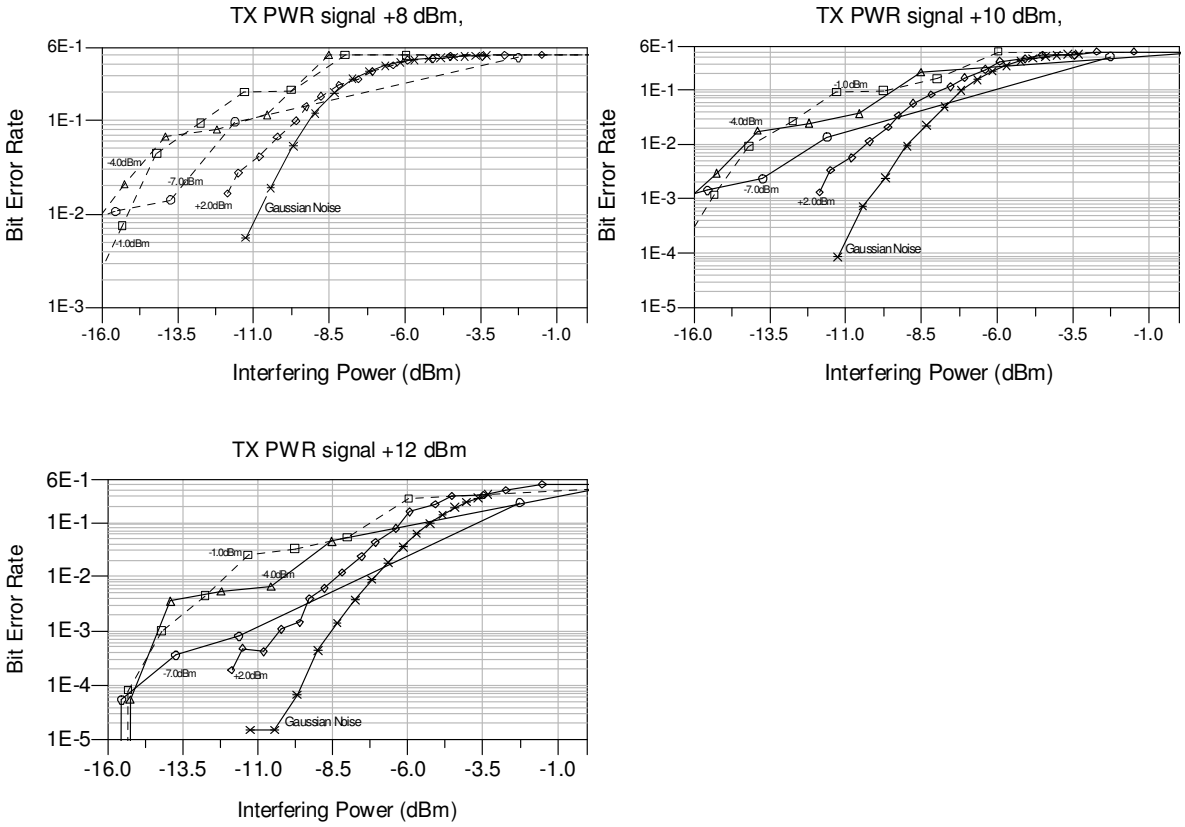

Fig. 50. Comparison of BER statistics as a function of the total interfering power (Gaussian noise and NL generated noise) for different excitation levels of Signal generator and NL source

The previous conclusion can be explained by the different signal affectation by noise along its bandwidth. Being the signal highly sensitive to its phase and amplitude modulation, different levels of affectation of the high and low signal frequency bands will cause higher impact than a over band constant density noise (white noise). On next Fig. 51 is illustrated the reason explained. Three different interferer saturation PA levels are represented

(interferer PA input power levels of 2dBm, -4dBm and -10dBm) and an example of the white noise power density level equivalent for the under consideration bandwidth.

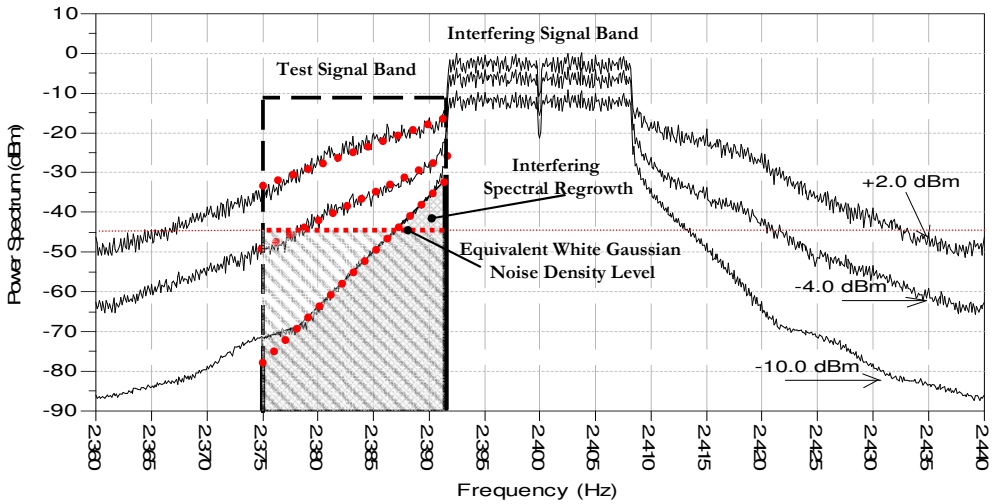

Fig. 51. Power spectrum illustration comparison from different interfering output PA saturation levels

The two different shaded areas represent the same total energy affecting the under test transmitted signal. As explained above, the two kind of interfering signals are considered as uncorrelated to the transmitted signal. This assumption would lead to expect similar performance when a signal is affected by white Gaussian noise or adjacent channel non correlated spectral regrowth nonlinear products. In Fig. 52 it can be verified the case of nearest possible adjacent channel interfering on the signal on where is notorious the impact in received signal spectrum.

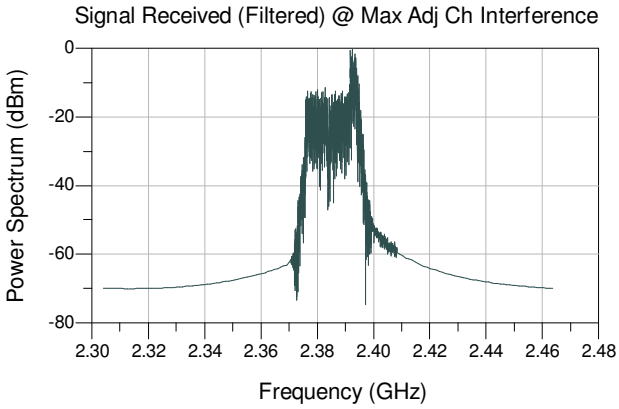

Fig. 52. Power spectrum visualization example at the receiver input for the case of minimum carrier frequency separation

Chapter 6

Conclusion

Despite the focus on a system level perspective analysis, this work had the necessity to dive into lower circuit representation levels to understand and achieve the results with the appropriate accuracy. The necessary broadness scope of the proposed study required a focused approach analysis on each of the constituent subjects involved. These analyses conducted to a selection of technology solutions capable of achieving the proposed objectives.

Engineering work is frequently distinguished by its trade-offs. On this work are focused the power efficiency versus spectral efficiency firstly apparent on the inband impact analyses (Sections 5.1 and 5.2). The higher error level margins from the 802.11b DQPSK (low spectral efficient) modulated signal allow higher in-band distortion levels. This fact turns in that this system can be operated at higher PA compression levels, limited primarily by out of band nonlinear products. Therefore, the possibility to increase the system output power and power added efficiency is opened. This PAE counter-balances with the high spectral efficiency achieved by the compared M-QAM OFDM 802.11a. In turn, the OFDM system was observed being as primarily limited by its in-band distortion levels requiring PA output power back off and, consequently, power efficiency reduction, to avoid higher unrecoverable signal phase distortion levels.

Also to notice the verification that the distortion impact is not only dependable from the signal RMS value but also by its instantaneous power levels, measured by its statistical variation values. In particular, the phase and amplitude distortion generated by higher compression levels of power amplifiers are correlated with the signal peak to average ratio characteristic. Additionally, the signal shaping will also influence the adjacent channel interference, particularly by the output signal shaping filters.

Nowadays, systems are full digitally controlled. The powerful real time processing units allow the increase of the "adaptable system" concept, exemplified by the herein studied modulation algorithms. Nevertheless, regarding the channel access method, the 802.11 systems are carrier sense induced, i.e., this system only transmits when the channel band is "silent". Results from Section 5.3 shows that possible newer optimized channel access strategies could be gainful if exploring the advantages of operating the PA on higher saturation levels. This would lead to higher power consumption efficiency supported by using the carrier frequency adaptable potential of digital systems and OFDM modulation. This strategy promotes a different philosophy considering "living with and exploring the nonlinearities drawbacks" for the case of contiguous band multichannel systems such as 802.11a. Additionally, a new concept of "band clear" could be re-defined in accordance to the performance required and propagation channel considerations. This adaptable system strategy technique is actually a hot subject studied and discussed by researchers as Cognitive Radio on the perspective of spectrum management efficiency.

This work has shown how to make possible the prediction of the behavior of a real characterized power amplifier when excited with a real complex modulated signal. The strategy adopted enables an engineer to make a better selection of the equipment/device specifications to be used by having a pre-estimation of what would be the system output when fully integrated. These techniques are of key importance when designing high performance circuits that demands carefully detail considerations and a close link to the real world device's performance.

References

[1] H. Brachtendorf, G. Welsch, R. Laur and A. Bunse-Gerstner, "Numerical Steady-State Analysis of Electronic Circuits Driven By Multi-Tone Signals", Electrical Engineering: 79, pp.103-112, 1996.

[2] J. Roychowdhury, "Analyzing Circuits with Widely Separated Time Scales Using Numerical PDE Methods", IEEE Trans. on Circuits and Systems - I, vol. CAS-48, pp.578-594, May 2001.

[3] J. C. Pedro and N. B. Carvalho, "Simulation of RF Circuits Driven by Modulated Signals Without Bandwidth Constraints", IEEE MTT-S Inter. Microwave Symp. Dig. CD-ROM, Seattle, Jun. 2002.

[4] J. C. Pedro and N. B. Carvalho, "Intermodulation Distortion in Microwave and Wireless Circuits", Artech House, Inc. Norwood, MA, Aug. 2003.

[5] Edward A. Lee, "Overview of the Ptolemy Project", Technical Memorandum No. UCB/ERL M03/25, University of California, Berkeley, CA, 94720, USA, July 2, 2003.

[6] The Berkeley Ptolemy Project Public Website: *http://ptolemy.eecs.berkeley.edu/*

[7] D. Sharrit, "New Method of Analysis of Communication Systems", MTT-S Nonlinear CAD Workshop, Jun. 1996, unpublished.

[8] V. Rizzoli, A. Neri and F. Mastri, "A Modulation-Oriented Piecewise Harmonic-Balance Technique Suitable for Transient Analysis and Digitally Modulated Signals", 26th European Microwave Conf. Proc.. pp.546-550, Prague, Sep. 1996.

[9] E. Ngoya and R. Larchevèque, “Envelope Transient Analysis: A New Method for the Transient And Steady-State Analysis of Microwave Communications Circuits and Systems”, IEEE MTT-S Inter. Microwave Symp. Dig., pp.1365-1368, San Francisco, Jun. 1996.

[10] M. Condon and E. Dautbegovic, “A Novel Envelope Simulation Technique for High-Frequency Nonlinear Circutis”, 33rd European Microwave Conf. Proc., pp.619-622, Munich, Oct. 2003.

[11] E. Ngoya, J. Sombrin and J Rousset, “Simulation des circuits et systémes: méthodes actuelles et tendances,” in Séminaires Antennes Actives et MMIC, Arles, France, April 1994, pp. 171–176.

[12] D. Sharrit, “Method for simulating a circuit,” US patent #5588142, Hewlett-Packard, Palo Alto, Calif., Application Filed: May 12, 1995, Santa Rosa, Calif.

[13] Nuno B. Carvalho, José C. Pedro and Michael B. Steer “Nonlinear Simulation of Mixers for Assessing System-Level Performance”, International Journal of RF and Microwave Computer-Aided Engineering, Vol. 15, Issue 4, July 2005, pp. 350-361.

[14] N. B. Carvalho, J. C. Pedro, W. Jang, M. B. Steer “Simulation of Nonlinear RF Circuits Driven By Multi-Carrier Modulated Signals”, IEEE MTT-S Inter. Microwave Symp, Long beach, California, June 2005

[15] Nuno B. Carvalho, José C. Pedro, Wonhoon Jang and Michael B. Steer “Nonlinear RF Circuits and Systems Simulation when Driven by Several Modulated Signals”, submitted to IEEE - MTT transactions 2005

[16] R. Nee and R. Prasaad, “OFDM wireless multimedia communications”, Artech House, Inc., Norwood, 2000.

[17] J. B. Dennis, First Version Data Flow Procedure Language, Technical Memo MAC TM61, May 1975, MIT Laboratory for Computer Science.

[18] Khaled M. Gharaibeh, Kevin G. Gard and Michael B. Steer,"In-Band Distortion of Multisines", IEEE Transactions on Microwave Theory and Techniques, Vol. 54, No. 8, August 2006

[19] Bussgang, J.J.; Ehrman, L.; Graham, J.W. "Analysis of nonlinear systems with multiple inputs", Proceedings of the IEEE Volume 62, Issue 8, Aug. 1974 Page(s):1088 - 1119

[20] E.F.T. Martijn, M.H.A.J. Herben, P.F.M. Smulders, M. Jevrosimovic and S.V. Savov, "Deliverable D2.1: State of the art channel models", Deliverable B4 Radio@hand project, pp. 1-45, 2002.

[21] Christian Olgaard , "Using advanced signal analysis to identify sources of WLAN transmitter degradations", *www.rfdesign.com*, October 2004

[22] Fager, Pedro, Carvalho and Zirath, "Prediction of IMD in LDMOS Transistor Amplifiers Using a New Large-Signal Model," IEEE Trans. On Microwave Theory and Techniques, Vol. 50, No. 12, pp. 2834-2842, December 2002.

[23] Cabral, P. M.; J. C. Pedro; NBC Carvalho; " Nonlinear device model of microwave power GaN HEMTs for high-power amplifier design ", IEEE Trans. on Microwave Theory and Tech. , Vol. 52 , No. 11 , pp. 2585 - 2592 , November , 2004

[24] van der Vorst, H.A.," Krylov subspace iteration", Computing in Science & Engineering, Vol. 2, Issue 1, Jan.-Feb. 2000 Page(s):32 - 37

[25] Issaount, A.; Kouki, A.B.; Ghannouchi, F.M., "Symbolically defined empirical large-signal model for HBTs compared to the Gummel-Poon model", Canadian Conference on Electrical and Computer Engineering, Vol. 1, pp. 31 – 34, May 2004.

[26] IEEE Std 802.11b-1999 (R2003), *http://standards.ieee.org*

[27] IEEE Std 802.11a-1999 (R2003), *http://standards.ieee.org*

[28] José L. Pino; Khalil Kalbasi, "Cosimulating Synchronous DSP Applications with Analog RF Circuits", Thirty-Second Annual Asilomar Conference on Signals, Systems, and Computers, November 1998.

[29] Avago Technologies, "ATF-55143 - Low Noise Enhancement Mode Pseudomorphic HEMT in a Surface Mount Plastic Package",http://www.avagotech.com

Appendices: 3D color plots from the simulation outputs from Chapter 5, Section 3.

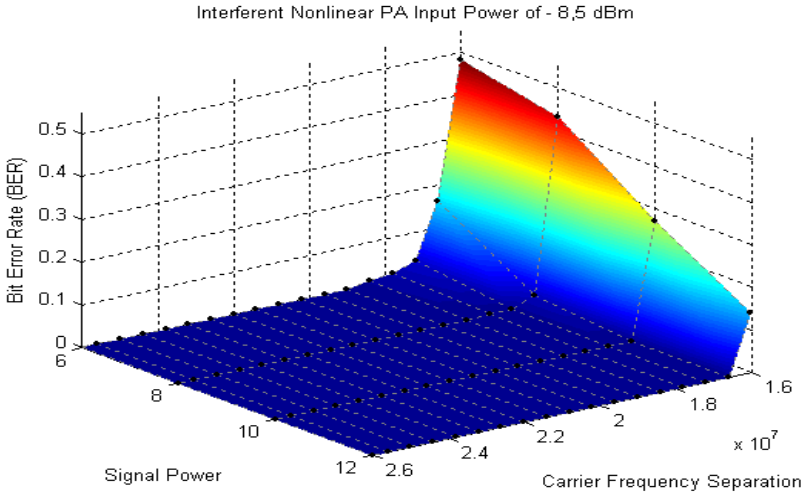

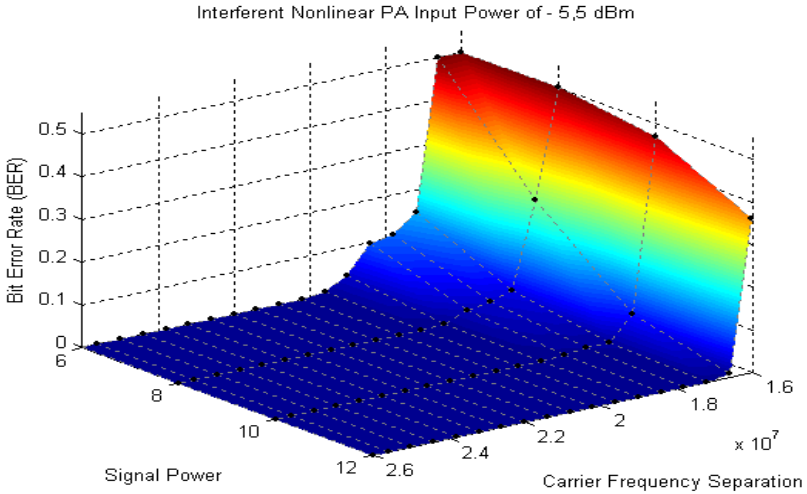

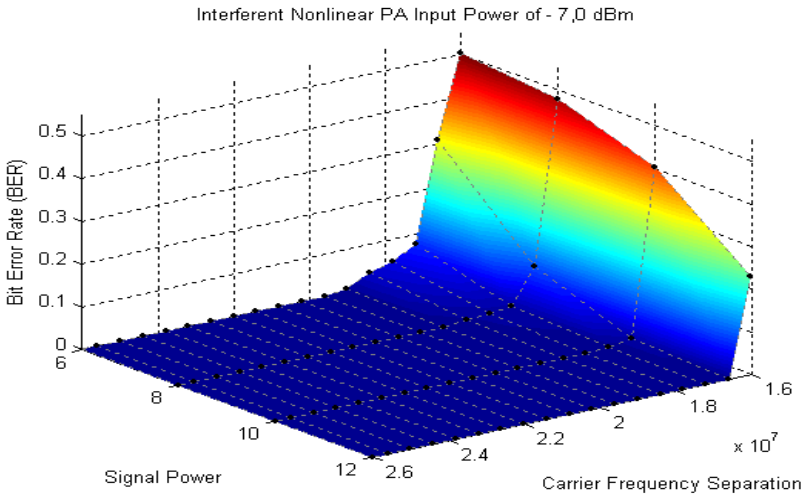

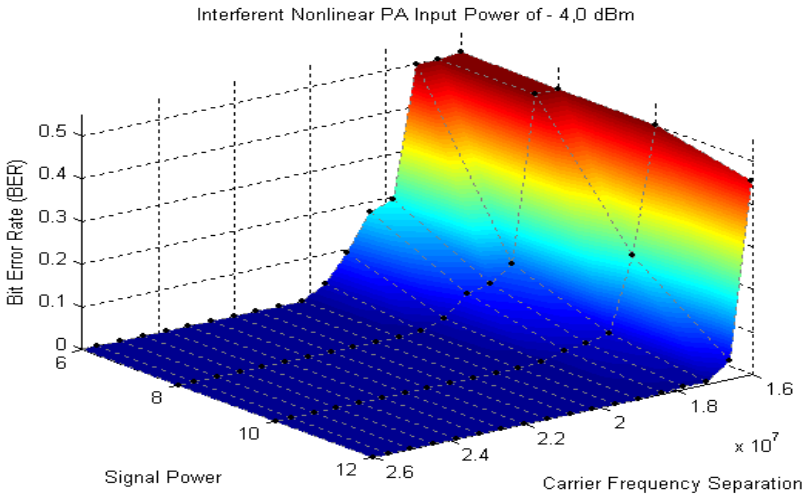

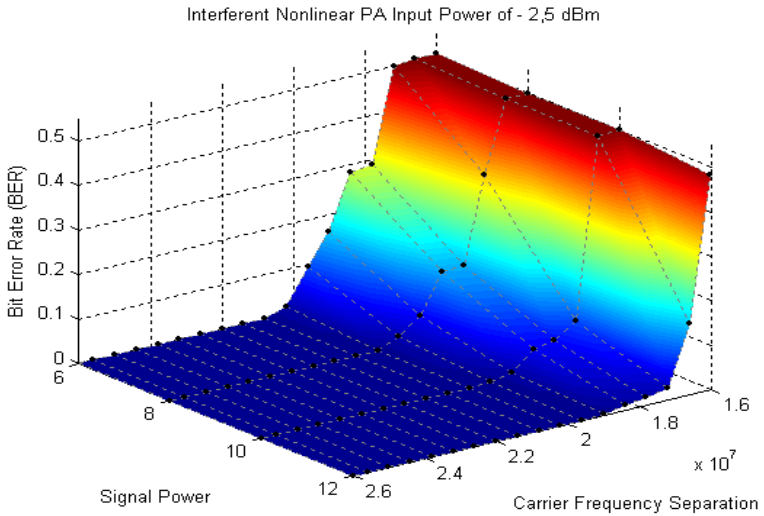
Interferent Nonlinear PA Input Power of - 2,5 dBm
Bit Error Rate (BER)
0
0.1
0.2
0.3
0.4
0.5
6
8
10
12
Signal Power
2.6
2.4
2.2
2
1.8
1.6
x 10^7
Carrier Frequency Separation

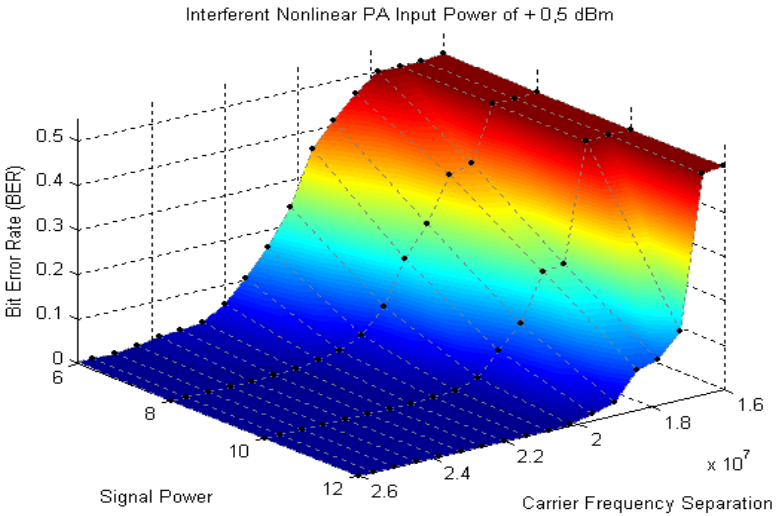
Interferent Nonlinear PA Input Power of + 0,5 dBm
Bit Error Rate (BER)
0
0.1
0.2
0.3
0.4
0.5
6
8
10
12
Signal Power
2.6
2.4
2.2
2
1.8
1.6
x 10^7
Carrier Frequency Separation

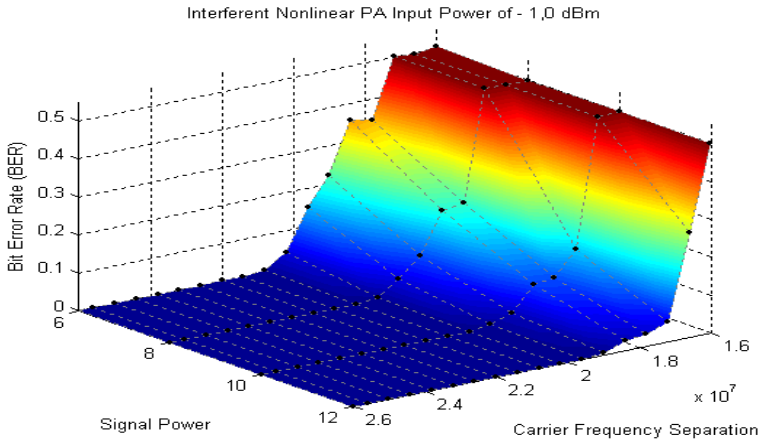
Interferent Nonlinear PA Input Power of - 1,0 dBm
Bit Error Rate (BER)
0
0.1
0.2
0.3
0.4
0.5
6
8
10
12
Signal Power
2.6
2.4
2.2
2
1.8
1.6
x 10^7
Carrier Frequency Separation

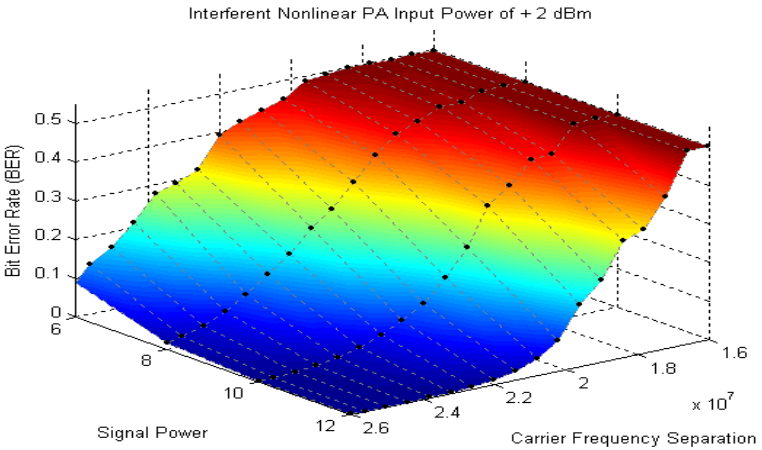
Interferent Nonlinear PA Input Power of + 2 dBm
Bit Error Rate (BER)
0
0.1
0.2
0.3
0.4
0.5
6
8
10
12
Signal Power
2.6
2.4
2.2
2
1.8
1.6
x 10^7
Carrier Frequency Separation